Cerebral Cortex February 2015;25:346–364
doi:10.1093/cercor/bht232
Advance Access publication August 22, 2013

Fine-Tuning of Neurogenesis is Essential for the Evolutionary Expansion of the Cerebral Cortex

Sylvie Poluch[1,2] and Sharon L. Juliano[1,2]

[1]Department of Anatomy, Physiology, and Genetics and [2]Department of Neuroscience, Uniformed Services University, Bethesda, MD, USA

Address correspondence to Sylvie Poluch, Department of Anatomy, Physiology, and Genetics, Uniformed Services University, 4301 Jones Bridge Road, Bethesda, MD 20814-4799, USA. Email: sylvie.poluch@usuhs.edu

We used several animal models to study global and regional cortical surface expansion: The lissencephalic mouse, gyrencephalic normal ferrets, in which the parietal cortex expands more than the temporal cortex, and moderately lissencephalic ferrets, showing a similar degree of temporal and parietal expansion. We found that overall cortical surface expansion is achieved when specific events occur prior to surpragranular layer formation. (1) The subventricular zone (SVZ) shows substantial growth, (2) the inner SVZ contains an increased number of outer radial glia and intermediate progenitor cells expressing Pax6, and (3) the outer SVZ contains a progenitor cell composition similar to the combined VZ and inner SVZ. A greater parietal expansion is also achieved by eliminating the latero-dorsal neurogenic gradient, so that neurogenesis displays a similar developmental degree between parietal and temporal regions. In contrast, mice or lissencephalic ferrets show more advanced neurogenesis in the temporal region. In conclusion, we propose that global and regional cortical surface expansion rely on similar strategies consisting in altering the timing of neurogenic events prior to the surpragranular layer formation, so that more progenitor cells, and ultimately more neurons, are produced. This hypothesis is supported by findings from a ferret model of lissencephaly obtained by transiently blocking neurogenesis during the formation of layer IV.

Keywords: corticogenesis, ferret, gyrencephaly, lissencephaly, subventricular zone

Introduction

The remarkable expansion of the cerebral hemispheres in humans is the result of increased neuron production during cortical development (Rockel et al. 1980; Dehay et al. 1993; DeFelipe et al. 2002). Other mechanisms occurring during postnatal development (such as dendritic arborization, gliogenesis, or intracortical myelination) are also involved, but to a lesser degree (Hill et al. 2010). A key evolutionary change in corticogenesis between smooth (lissencephalic) and convoluted (gyrencephalic) species is a protracted neurogenesis. Compared with rodents, neurogenesis is 3 times longer in ferrets and 10 times longer in primates (Noctor et al. 1997; Kornack and Rakic 1998; Martinez-Cerdeno et al. 2006). In gyrencephalic animals, prolonged neurogenesis produces a slower depletion of the cortical progenitor pool; an increase in cell cycle length is thought to be involved in this process (Kornack and Rakic 1998; Calegari et al. 2005; Lukaszewicz et al. 2005; Rakic 2005, 2009).

The recent discovery of 2 new classes of cortical progenitor cells, the intermediate progenitor (IP) cells (Haubensak et al. 2004; Miyata et al. 2004; Noctor et al. 2004) and the outer radial glia (oRG; Fietz et al. 2010; Hansen et al. 2010), stimulated a number of studies in this field (for review see Lui et al. 2011; Molnar 2011; Borrell and Reillo 2012). Comparative studies between lissencephalic and gyrencephalic species greatly helped our understanding of the mechanisms underlying cortical surface expansion (Smart et al. 2002; Martinez-Cerdeno et al. 2006, 2012; Reillo et al. 2011; Garcia-Moreno et al. 2012; Kelava et al. 2012). A complementary approach consists of comparing, within the same animal, regions that undergo different degrees of increased neuron production (Dehay et al. 1993; Smart et al. 2002). More recently, Reillo et al. (2011) show changes in mitotic cell density between the temporal cortex (relatively less gyrencephalic) and the parietal cortex (relatively more gyrencephalic) in cats and humans.

In the present study, we combine these 2 comparative approaches: Between different animal models and between 2 cortical regions within the same animal. We used 3 animal models: (1) Lissencephalic mouse, (2) gyrencephalic normal ferrets showing regional differences in gyrification (i.e. the parietal cortex expands more compared with the temporal cortex), and (3) moderately lissencephalic ferrets obtained by injecting an antimitotic, methylazoxy methanol acetate (MAM), on the 33rd day of development (E33), coinciding with the birth of layer 4 neurons in the parietal cortex (Rabe et al. 1985; Noctor et al. 1997). E33 MAM-treated ferrets display defects in γ-aminobutyric acidergic signaling and neuronal migration into the cerebral cortex (Poluch et al. 2008; Abbah and Juliano 2013) as well as an altered cortical lamination and brain morphology, which shows as a smoother appearance of the cerebral hemispheres (Rabe et al. 1985; Noctor et al. 1999). We demonstrate here that E33 MAM-treated ferrets present characteristics observed in normal ferrets of an expansive cortex as well as characteristics found in mice, both showing similarities in temporal and parietal cortical surface expansion.

By comparing corticogenesis between these 3 animal models (mice, normal ferrets, and lissencephalic ferrets) and within each animal model (parietal vs. temporal cortex), our goal is to better understand mechanisms underlying overall and regional cortical surface expansion. We chose to study 3 aspects of neurogenesis: The relative size of proliferating regions, and the distribution as well as the phenotype of dividing cells. Surprisingly, we found no fundamental differences between mice and ferrets. However, events observed during late neurogenesis in mice occur earlier in normal ferrets, prior to the formation of supragranular layers (i.e. E33). The significance of this time window appears essential for gyrification as MAM exposure at E33 alters the course of neurogenesis and results in moderately lissencephalic ferrets. Finally, comparing the developmental dynamics of the temporal and parietal

cortices, within the same animal model, shows that neurogenesis is more advanced in the temporal cortex in mice and E33 MAM-treated ferrets, while in normal ferrets, neurogenesis displays similar a degree of advancement in both regions.

Our results suggest that fine-tuning of neurogenesis is a key evolutionary mechanism, and that changes in the timing, rather than the sequence, of neurogenic events are essential for overall and regional cortical surface expansion.

Materials and Methods

Animals

Timed pregnant ferrets (*Mustella putorius*) were purchased from Marshall Farms (New Rose, NY, USA); ferret kits are born after 41 days of gestation. On the 24th (E24), 33th, or 38th (E38) day of embryonic (E33) development, pregnant ferrets, anesthetized with 5% isofluorane using a mask, were injected intraperitoneally (IP) with MAM (Midwest Research Institute, 14 mg/kg) diluted in a sterile saline buffer. E25 (normal), E33 (normal), and E35 (normal and E33 MAM-treated) embryos were obtained by caesarean section using isofluorane anesthesia under the supervision of a veterinarian. We also used normal and MAM-treated postnatal day 0 (P0), P7, P14, and adult (6 months and older) ferrets that were anesthetized with an IP injection of pentobarbital sodium (50 mg/kg) prior to brain removal. C57BL/6 mice were purchased from The Jackson Laboratory (Bar Harbor, ME, USA) and bred in the Uniformed Services University (USU) animal facilities. Timed pregnant dams were anesthetized with an IP injection of pentobarbital sodium (50 mg/kg) on the embryonic day 12, 14, 16, or 18 (plug day was embryonic day 0). Embryonic brains were fixed by immersion in a solution of phosphate buffered containing paraformaldehyde (4%) and sucrose (4%); postnatal brains were intracardiacally perfused with the same fixative solution. The cryoprotected brains were stored in a −80 °C freezer and, subsequently, sectioned at 25 µm using a LEICA cryostat. Cryostat sections were air dried and stored in a −20 °C freezer. The use of animals and the methods of this study were approved by the Institutional Animal Care and Use Committee (IACUC) at USU and under Animal Welfare Assurance number A3448-01. The experiments were performed at an AAALAC accredited institute.

Fluorescence Immunocytochemistry

Antigen-retrieval procedure was performed by incubating cryostat sections for 30 min in a 90 °C solution of 10 mM citrate buffer (pH 6.0) (Thermo Scientific) placed in an Isotemp digitial-control water bath (Fisher Scientific, Pittsburg, PA, USA) set at 90 °C. The sections were then transferred to a room temperature (RT) solution of 10 mM citrate buffer and immediately placed 5 min at 4 °C. After washes in phosphate buffered saline (PBS) (4 × 10 min) at RT, the slices incubated for 1 h (also at RT) in a buffer containing: PBS, Triton X-100 (0.1%), goat serum (3%), and bovine serum albumin (2%). The primary antibodies were diluted in the same buffer, and the cryostat sections were incubated overnight at 4 °C. The following primary antibodies were used: Mouse IgG monoclonal antibodies against Pax6 (1/100, Hybridoma Bank), mouse IgG monoclonal antibodies against Tau1 (1/200, Millipore), rabbit polyclonal antibodies against Tbr2 (1/1000, Abcam), and rat polyclonal phospho-histone-3 (PH3; 1/1000, Abcam). After washes in PBS, the corresponding secondary antibodies were used: Anti-rat IgG Alexa 350, antirabbit IgG Alexa-488, and antimouse IgG Alexa-546 (1/200, Invitrogen). Finally, the sections were washed in PBS and mounted in Mowiol. For the acquisition of fluorescence images, we used an Axiovert 200 microscope (Zeiss) equipped with an Apotome and Axiovision 4.7.

Western Blot

Protein samples were obtained from cortices of 3 newborn normal ferrets and 3 E33 MAM-treated newborn ferrets. The tissues were snap-frozen, stored at −80 °C, and subsequently, homogenized in cold lysis buffer (20 mM Tris buffer, pH 7.5, 150 mM NaCl, 1% Triton X-100, 0.1% sodium dodecyl sulfate, and 1 mM ethylenediaminetetraacetic acid) in the presence of protease inhibitors (Complete; Roche Molecular Biochemicals) and sonicated on ice. Proteins were separated by electrophoresis on 3–8% Tris-acetate gels (NuPage Novex, Invitrogen) and transferred onto nitrocellulose membranes (IBot, Invitrogen). After washes (3 × 10 min) at RT in TBS–Tween20 (0.1%), the membranes were incubated for 1 h (also at RT) in a membrane blocking buffer solution (Invitrogen), and then overnight at 4 °C in a blocking buffer solution containing the following primary antibodies: Mouse IgG monoclonal antibodies against Pax6 (1/500, Hybridoma Bank), rabbit IgG polyclonal antibodies against Tbr2 (1/2000, Abcam), and rabbit polyclonal BLBP (1/1000, Abcam). After washes in TBS–T, the membranes were incubated at RT for 2 h with the appropriate peroxidase-conjugated secondary antibodies: Goat antimouse IgG or goat antirabbit IgG (1/1000, Thermo Scientific). Results were visualized using a Fugi System. Densitometry analysis was achieved using the ImageJ software. Results were averaged from 2 independent experiments.

Calculation of the Gyrification Index

The gyrification index (GI) is a quantitative calculation of the degree of cortical folding obtained by comparing the length of the pial surface with the length of the outer cortical contour (Zilles et al. 1989). The calculations of GI in normal and E33 MAM-treated adult ferrets were performed on 25-µm thick cryostat coronal sections counterstained with bisbenzimide. Sections containing the following gross structures were selected: The cruciate sulcus, coronal sulcus, suprasylvian and pseudosylvian sulci, as well as the anterior commissure (Juliano et al. 1996; McLaughlin et al. 1998; Noctor et al. 2001) (Fig. 1*A*,*B*). We used a ×5 objective to acquire mosaic images, which were merged into a single image. For each merged picture, the pial surface was outlined in red and the outer cortical contour outlined in green using PowerPoint; an example is shown in drawing 1 of Figure 1. Lengths (in pixels) of red and green lines were measured using an ImageJ. For each slice, the GI was measured as follows: GI = length of red line/length of green line. In addition to the overall GI, a regional GI was calculated for the primary somatosensory (SI) cortex (region between the cruciate and coronal sulci) and for the anterior sylvian cortex (AS; region between suprasylvian and pseudosylvian sulci). In this case, the regional GI was obtained by comparing the length of the pial surface lining the cortical region of interest with that of the outer cortical contour lining the same region. Drawing 2 of Figure 1 shows how the SI GI was calculated; similar method was used for the calculation of the AS GI.

Quantification of the Size of the Proliferating Zones

The size of the different proliferating zones was measured using Pax6 and Tbr2 immunostaining in combination with nuclear (bisbenzimide) staining. The following criteria were used to delineate each region: (1) The ventricular zone (VZ) is a proliferative region lining the lateral ventricle by a high-cell density and a strong Pax6 expression. (2) The subventricular zone (SVZ), located between the VZ and the intermediate zone (IZ), presents a lesser cell density compared with the VZ (but greater compared with the IZ) and strong Tbr2 expression. Starting at E16 in mice and E33 in ferrets, the SVZ can be subdivided into an inner and outer compartment. The inner SVZ (ISVZ) and outer SVZ (OSVZ) are easily outlined based on differences in cell density (the ISVZ being denser than the OSVZ) (Supplementary Fig. 4*A*,*C*). Results were confirmed on adjacent slices using nuclear staining combined with antibodies against Tbr2 and Tau1 as described by Martinez-Cerdeno et al. (2012) (Supplementary Fig. 4*B*,*D*). We used a ×25 objective to acquire multiple z-stack images (3 z-sections, with a 2-µm interval), which were collapsed into a single image. The relative size of the VZ and SVZ were measured (in µm) on each collapsed image using ImageJ and expressed as a percentage of the cortical wall thickness.

Quantification of the Distribution and Phenotype of Dividing Cells

The distribution and phenotype of dividing cells, visualized using antibodies against phospho-histone-3 (PH3), were analyzed in the VZ and inner and outer SVZ. PH3+ cells located in the cortical plate and the

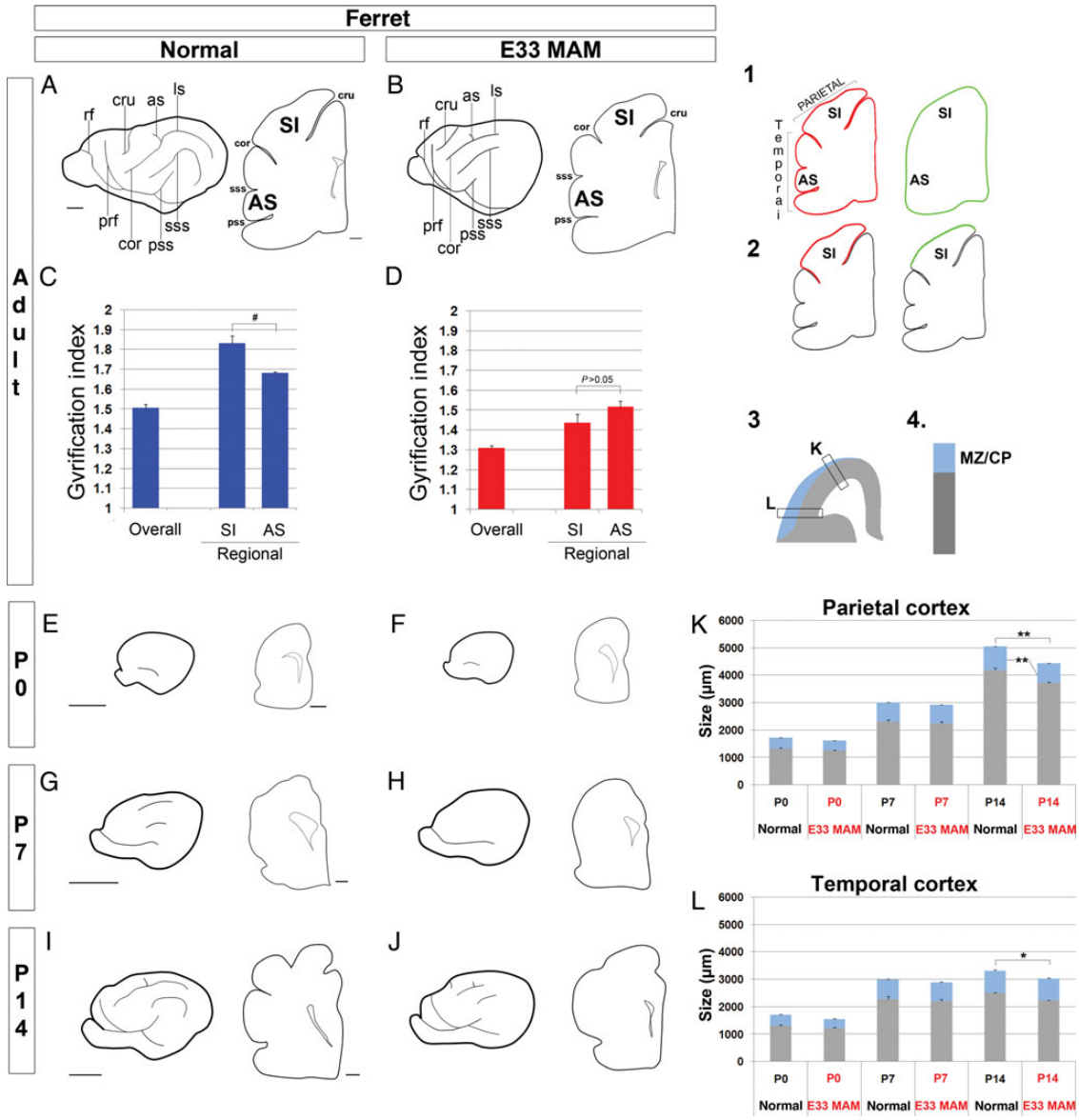

Figure 1. Sulcal formation and cortical growth during postnatal development in normal and E33 MAM-treated ferrets. Normal ferrets are shown on the left panel and E33 MAM-treated ferrets on the right. For each age, adults (*A* and *B*), P0 (*E* and *F*), P7 (*G* and *H*), and P14 (*I* and *J*), one drawing represents the lateral aspect of the left cerebral hemisphere, while the other drawing represents a coronal slice taken at the level of the anterior commissure. GI in normal (*C*) and E33 MAM-adult ferrets (*D*). Examples of drawings used to calculate the overall GI (1), and regional GI in the primary SI cortex (2) of a normal adult ferret. The red line represents the pial surface and the green line represents the outer cortical contour. GI = (length of red line/length of green line). Three normal and 3 E33 MAM-treated adult ferrets were used to calculate the GI; for each animal, results are averaged from 3 slices. $^{**}P < 0.001$ and $^{*}P = 0.01$ (normal compared with E33 MAM-treated ferrets), $^{\#}P = 0.005$ (SI cortex compared with AS cortex); *t*-test. Scale bar: 1000 μm (hemisphere) and 500 μm (coronal slice). (*K* and *L*) Cortical growth was measured in the normal and E33 MAM-treated cortex from P0 to P14 using coronal slices with nuclear staining. The sizes of the cortical wall including the MZ/CP (see drawings 3 and 4) in the parietal cortex are shown in graph (*K*) and for the temporal cortex in graph (*L*). Three normal and 3 E33 MAM-treated adult ferrets were used for quantification; for each animal, results are averaged from 3 slices. $^{**}0.007 < P < 0.010$, $^{*}P = 0.027$; *t*-test. as, ansinate sulcus; cor, coronal sulcus; cru, cruciate sulcus; ls, lateral sulcus; prf, presylvian fissure; pss, pseudosylvian sulcus; rf, rhinal fissure; sss, suprasylvian sulcus; SI, primary somatosensory cortex; AS, anterior sylvian cortex; CP, cortical plate; MZ, zone marginal.

marginal zone were not included in our study as progenitor cells from these regions differ in their molecular characteristics, origin, and identity of their clonal progeny from progenitor cells isolated from the VZ and SVZ (Costa et al. 2007). In addition to PH3 immunostaining, we used antibodies against Pax6 and Tbr2 to determine the boundaries between the proliferating regions as described above; results were confirmed on adjacent sections stained with bisbenzimide. PH3 immunostaining was not used to determine the boundaries; however, we observed that the VZ contains a row of PH3+ cells lining the lateral ventricle, and that the lower limit of the SVZ is delineated by a distinct row of abventricular PH3+ cells (Bayer et al. 1991; Brazel et al. 2003). We used a ×25 objective to acquire multiple z-stack images (3 z-sections, with a 2-µm interval), which were collapsed into a single image. On each collapsed image, the number and phenotype (i.e. Pax6+, Tbr2+, or both) of PH3+ cells were assessed in the VZ, inner SVZ, and outer SVZ. Quantifications were performed manually in Photoshop in a 200-µm wide section; results are expressed as a percentage.

Statistical Analysis

For each age and group (mice, normal ferrets, or E33 MAM-treated ferrets), 3 animals were analyzed. For each animal, data obtained in the parietal and temporal cortex were averaged from 2 to 3 slices taken at the level of the anterior commissure. Appropriate tests [*t*-test or 2-way analysis of variance (ANOVA) followed by a Holm-Sidak test] were

conducted for statistical difference using SigmaStat (Systat Software, Inc.); *P*-values of <0.05 are considered statistically significant.

Results

Cortical Surface Expansion in Normal and E33 MAM-Treated Ferrets

Lissencephaly can be experimentally induced in ferrets by injecting the antimitotic MAM on the 33rd day of embryonic development (E33) (Fig. 1*A*,*B*; Rabe et al. 1985; Noctor et al. 1999). E33 corresponds to the production of layer 4 neurons in the primary SI (Noctor et al. 1997). Differences in the degree of cortical folding in normal versus E33 MAM-treated adult ferrets were quantified by measuring the GI on coronal slices taken at the level of the anterior commissure; this level includes SI (Fig. 1*A*,*B*). GI, as defined by Zilles et al. (1989), is a quantitative calculation obtained by comparing the length of the pial surface with that of the outer cortical contour (drawing 1 of Fig. 1). The overall GI is greater in normal adult ferrets compared with E33 MAM-treated animals ($P < 0.001$) (Fig. 1*C*,*D*). We also measured the GI of specific regions in the parietal cortex (SI) and in the temporal cortex (AS) (drawing 2 of Fig. 1). In normal ferrets, the GI is greater in SI compared with the GI in the AS (Fig. 1*C*). In E33 MAM-treated ferrets, the GI decreases in both parietal and temporal regions ($P < 0.001$, compared with normal), and SI GI is not significantly greater than AS GI ($P > 0.05$; Fig. 1*D*). This is similar to a mouse brain, although E33 MAM-treated ferrets are not fully lissencephalic since they display an overall GI of 1.3 compared with 1.03 in mouse (Hevner and Haydar 2012).

Sulcal Formation and Cortical Growth in Normal and E33 MAM-Treated Developing Postnatal Ferrets

Because decreased GI after MAM injection reflects abnormal cortical development, we compared gross brain anatomy of normal and E33 MAM-treated postnatal ferrets. We first assessed sulcal formation. In normal ferrets, gyrification occurs postnatally (Smart and McSherry 1986; Jackson et al. 1989) and is complete at P28 (Neal et al. 2007). To study how this process alters after MAM exposure, we compared the formation of sulci on the lateral aspect of cerebral hemisphere and using coronal slices, taken at the level of the anterior commissure, in normal and E33 MAM-treated postnatal ferrets from P0 to P14 (Fig. 1*E*–*J*).

At birth (P0), ferret brains are mostly lissencephalic (Jackson et al. 1989; Neal et al. 2007); the rhinal sulcus is visible in the ventro-lateral region of the hemisphere in both normal and E33 MAM-treated ferrets (Fig. 1*E*,*F*). One week after birth (P7), in normal ferrets, the rhinal sulcus extends anteriorly and posteriorly, and the coronal, lateral, as well as suprasylvian sulci are visible on the lateral aspect of the cerebral hemisphere; sulcal indentations are perceptible on coronal sections (Fig. 1*G*). In contrast, E33 MAM-treated brains remain primarily lissencephalic (the rhinal sulcus is the only discernible sulcus, Fig. 1*H*). Two weeks after birth (P14), the presylvian, cruciate, ansinate, and pseudosylvian sulci are visible on the lateral aspect of the hemisphere in both normal and E33 MAM-treated ferrets; however, coronal sections show that sulcal indentations are not as deep in E33 MAM-treated ferrets compared with normal (Fig. 1*I*,*J*). Further maturation occurs in both normal and MAM-treated ferrets, but adult E33 MAM-treated ferrets do not reach the normal degree of cortical folding (Fig. 1*A*,*B*).

Next, we compared cortical growth in normal and E33 MAM-treated postnatal ferrets. The size (in μm) of the cortical wall and cortical plate were measured in the temporal and parietal cortices from P0 to P14 using coronal slices counterstained with bisbenzimide. Although the cortical wall thickness is slightly smaller at P0 and P7 after MAM injection, the overall size is not significantly different compared with normal until P14 (in both temporal and parietal cortices) (Fig. 1*K*,*L*). The size of the cortical plate is significantly decreased (compared with normal) at P14 in the parietal cortex (Noctor et al. 2001; Fig 1*K*), but not in the temporal cortex (Fig. 1*L*).

In conclusion, MAM treatment at E33 alters sulcal formation and cortical growth. In addition, defects are greater in the parietal compared with temporal region.

Spatio-temporal Effects of MAM

Differences in the effects of MAM in the temporal versus parietal cortex are the result of the latero-dorsal gradient of cortical development; at E33, the temporal region is relatively more mature compared with the parietal region. MAM toxicity is, indeed, greater when the injection occurs during early stages of development. For example, MAM exposure on the 24th day of embryonic development (E24; when the subplate neurons and layer 6 neurons are being generated in the parietal cortex; Noctor et al. 1997) is associated, at birth, with smaller brains and the absence of the rhinal sulcus compared with normal (Supplementary Fig. 1*A*–*D*). The parietal cortex of newborn E24 MAM-treated shows a significant reduction in the size of the cortical wall and cortical plate compared with normal (Supplementary Fig. 1*E*). Here, again the temporal cortex is less affected: Although the cortical plate is significantly reduced compared with normal, the overall cortical thickness is not significantly different (Supplementary Fig. 1*F*). Note that data after P0 are not presented as E24 MAM-treated kits are not viable and die 24–48 h after birth. When MAM is injected during later stages of neurogenesis at E38 (which corresponds to the production of layer 2 neurons in the parietal cortex; Noctor et al. 1997), cortical growth (Noctor et al. 2001) and GI (Supplementary Fig. 2) are not significantly altered compared with normal.

In addition to the latero-dorsal gradient of development, cortical development follows a rostro-caudal gradient, so that the visual cortex is relatively more immature compared with the parietal cortex. MAM exposure at E33 alters the production of layer 4 neurons in the parietal cortex and layer 5 neurons in the visual cortex (Noctor et al. 1997). As a result, the effects of MAM are more severe in the visual cortex compared with the parietal cortex (Noctor et al. 1997; Fig. 1*A*,*B* and Supplementary Fig. 3*A*,*B*). (1) The adult cerebral cortex at the level of the visual cortex is fully lissencephalic (with an enlarged lateral ventricle) compared with moderately lissencephalic at the level of the parietal cortex (Fig. 1*C*,*D* and Supplementary Fig. 3*C*), and (2) in the visual cortex, the size of the cortical wall and cortical plate are significantly different starting at P7 compared with normal (Supplementary Fig. 3*L*) (vs. P14 in the parietal cortex; Fig. 1*K*). Note that in the normal ferret, gyrification is lesser at the level of the visual cortex compared with that of the parietal cortex (Supplementary Fig. 3*C* and Fig. 1*C*).

Rationale and Approach

Studied together, mice, normal, and lissencephalic ferrets provide further insights into (1) overall cortical expansion (by comparing gyrencephalic vs. lissencephalic brains) and (2)

regional cortical expansion (by comparing parietal vs. temporal cortices). To achieve these goals, we focused our study on cortical development and more particularly neurogenesis; 3 neurogenic parameters were selected. These included the size of proliferating regions, the distribution and phenotype of actively cycling cells. First, we compared the developmental dynamics in the parietal cortex (presumptive SI cortex) between each animal model. We chose this cortical region, because it demonstrates a different GI in the 3 adult animal models that range from: Null (lissencephalic mouse; GI = 1.03; Hevner and Haydar 2012), intermediate (E33 MAM-treated ferrets; GI = 1.43), and to uttermost (normal ferrets; GI = 1.83) (Fig. 1*C*,*D*). Secondly, we compared the developmental dynamics in the parietal and temporal cortices within each animal model. We chose these 2 regions because they reach a different degree of gyrification in normal adult ferrets, unlike in adult mice or adult E33 MAM-treated ferrets (Fig. 1*C*,*D*). Finally, we chose 4 developmental stages to span the period of neuron production from lower to upper cortical layers: Stage 1 (formation of subplate cells and layer 6), stage 2 (formation of layer 4), stage 3 (formation of lower layer 2), and stage 4 (formation of upper layer 2). These developmental stages correspond to the following embryonic (E) and postnatal (P) days: E12, E14, E16, and E18 in mice (Angevine and Sidman 1961; Smart and Smart 1982; Caviness et al. 1995) (Fig. 2*A*,*B*) and to E25, E33, P0, and P7 in ferrets (Noctor et al. 1997) (Fig. 2*C*,*E*).

Development Dynamics of the VZ and SVZ

To study the magnitude of proliferating zones, we outlined the VZ and the SVZ using nuclear staining combined with antibodies against Pax6 and Tbr2 (Fig. 2 and Supplementary Fig. 4). The overall size (in µm) of the cortical wall is not altered until the end of neurogenesis (P14) in E33 MAM-treated ferrets compared with normal (Fig. 1*K*,*L*). However, significant differences in the size of the VZ and SVZ are observed at P0 and P7 (Supplementary Fig. 5). Therefore, to compare their developmental dynamics in normal versus E33 MAM-treated, the sizes of the VZ and SVZ are normalized to the overall cortical wall thickness and expressed as a percentage.

To better understand the contribution of the VZ and SVZ in overall cortical surface expansion, we compared their size during neurogenesis in the mouse and ferret parietal cortex (Figs 2*B*,*E*,*F* and 3*A*–*I*). The VZ is the largest proliferating region in mouse until E15.5, while in normal ferrets, the SVZ is larger than the VZ starting at E31 (equivalent to E13.5 in mice) (Fig. 3*A*,*B*). Although the SVZ remains the largest of the 2 proliferating regions after MAM treatment, it is significantly reduced compared with normal ($P < 0.001$, Fig. 3*C*). To better compare normal and E33-MAM treated ferrets see Supplementary Figure 6. In accordance with previous studies, we show that SVZ expansion is essential for overall cortical surface expansion (Smart et al. 2002; Zecevic et al. 2005; Martinez-Cerdeno et al. 2006).

Next, we explored the contribution of the VZ and SVZ in regional cortical surface expansion by comparing how temporal and parietal sizes evolve during neurogenesis for each animal model (Figs 2 and 3*D*–*I*). First, we found that the developmental dynamics of the VZ follow a similar trend in mice and normal ferrets (Fig. 3*G*,*H*). The VZ is significantly larger in the parietal cortex up to E16 in mice and up to E33 in ferrets, compared with the temporal cortex. Because no fundamental differences are observed between the 2 species, we conclude that the expansion of the ferret parietal cortex does not rely on VZ expansion.

Next, we examined the developmental dynamics of the SVZ. Compared with the temporal SVZ, the parietal SVZ is larger in mice at the end of neurogenesis (E18), while in ferrets, it is equal (E25) or larger during most of its duration (from E33 to P7) (Fig. 3*D*,*E*). As previously reported by Kriegstein et al. (2006), cortical regions with a higher degree of gyrification display a significantly increased SVZ compared with regions with lesser gyrification. This agrees with our findings since at its maximal, the ferret SVZ represents about 30% of the cortical wall in the temporal cortex and 40% in the parietal cortex. In addition, the ferret parietal SVZ reaches its maximal size during the early stages of neurogenesis (E33—corresponding to layer 4 formation) compared with P0 in the temporal SVZ (corresponding to upper layer 2 formation) (Fig. 3*E*). Therefore, comparing the dynamics of proliferating regions along the latero-dorsal axis in mice and normal ferrets demonstrates (1) similarities for the VZ, (2) but major differences for the SVZ as in ferret the parietal SVZ grows prematurely and at substantially higher rates compared with the temporal SVZ. This suggests that SVZ expansion is essential for parietal gyrification in normal ferrets. This hypothesis was confirmed with lissencephalic ferrets. Indeed, MAM exposure at E33 prevents the parietal SVZ from expanding more than the temporal SVZ (Fig. 3*F*). Note that after MAM injection, the temporal and parietal VZ are both decreased (compared with normal) but to a similar degree (Fig. 3*I*); this reinforces the prevalence of the SVZ in ferret parietal expansion.

In summary, overall and regional cortical surface expansion correlate with the increased size of the SVZ. In addition to the magnitude, the timing of SVZ expansion is fundamental: The SVZ reaches its maximum earlier (1) in ferret compared with mice (E33 vs. E18; Fig. 3*A*,*B*) and (2) in the ferret parietal cortex compared with the ferret temporal cortex (E33 vs. P0; Fig. 3*E*).

Developmental Dynamics for the Inner and Outer SVZ

Because the SVZ can be further subdivided into an inner and outer compartment starting at E16 in mice and E33 in ferrets, we examined the developmental dynamics for each compartment (Fig. 3*J*–*R* and Supplementary Fig. 6*E*–*H*).

First, we explored whether the ISVZ and OSVZ differ when comparing the mouse and ferret parietal cortex. Overall, we found a similar trend between mice and normal ferrets, with the ISVZ being larger during early stages of neurogenesis and the OSVZ being larger during later stages of neurogenesis (Fig. 3*J*,*K*). However, the magnitude of the ISVZ and OSVZ differs between mice and normal ferrets. MAM exposure results in the reduction of both SVZ compartments at P0 (ISVZ, $P < 0.001$ and OSVZ, $P = 0.003$) and in the OSVZ only at P7 ($P = 0.048$) compared with normal (Fig. 3*L*). Here again, we observe a gradation of the effects induced by MAM depending on the timing of the injection as demonstrated by comparing the E24 MAM-treated and E33 MAM-treated ferret (Supplementary Fig. 1*G*–*L*). The reduction of the ISVZ and OSVZ (in µm and in % of the cortical wall) is the greatest in E24 MAM-treated ferrets compared with E33 MAM-treated and normal ferrets (Supplementary Fig. 1*M*,*N*). We conclude here that ferret

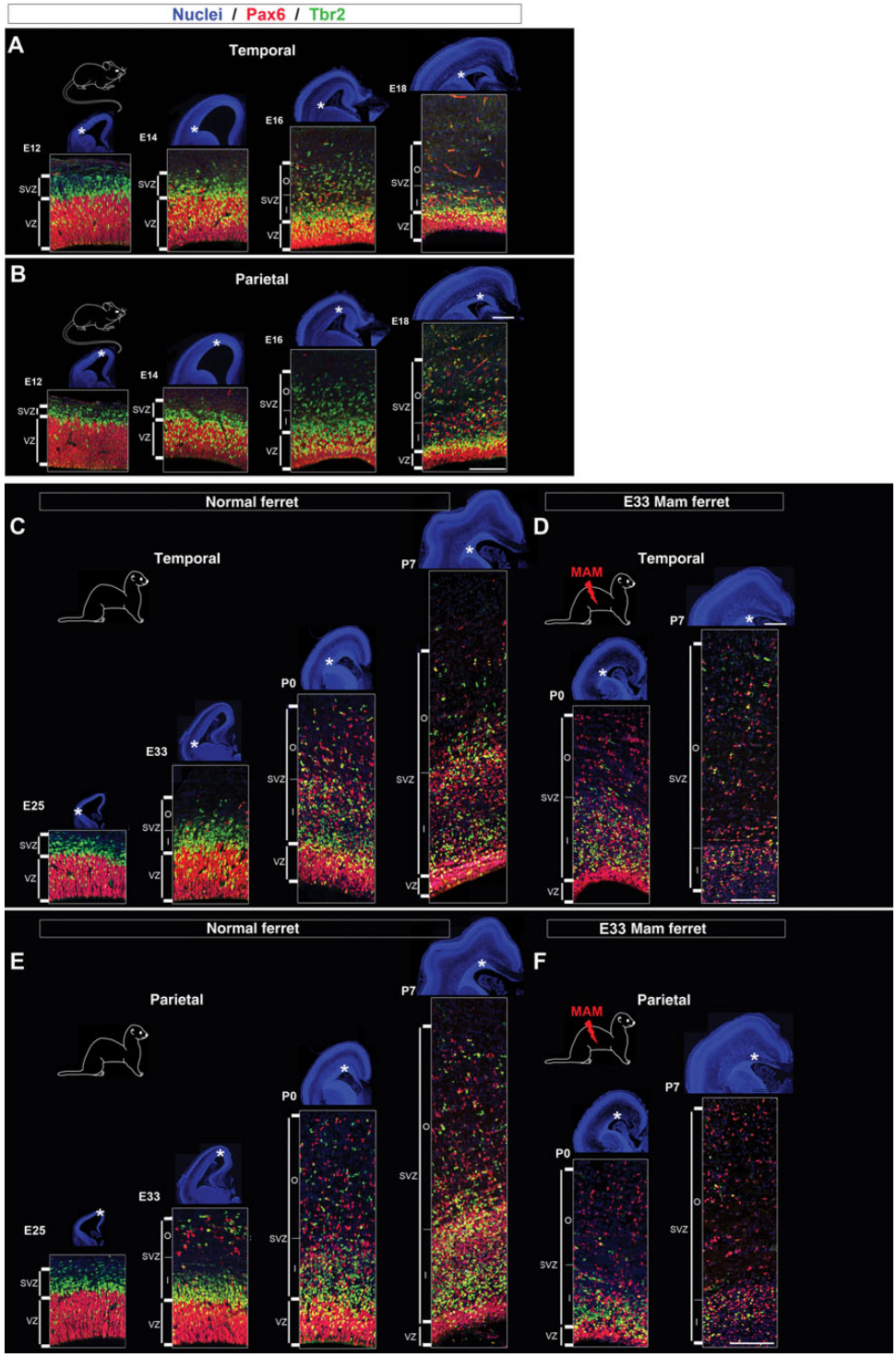

Figure 2. Proliferating zones in mouse, normal ferrets and E33 MAM-treated ferrets from early to late neurogenesis. Immunostaining against Pax6 (red) and Tbr2 (green) followed by nuclear counterstaining (blue). Low-magnification pictures (nuclear staining) show cortical growth in mouse from E12 to E18 (*A* and *B*), normal ferrets from E25 to P7 (*C*–*E*), and E33 MAM-treated ferrets from P0 to P7 (*D*–*F*). Higher magnifications of Pax6 and Tbr2 immunostaining are taken in the temporal and parietal cortices (as indicated by the asterisks). VZ, ventricular zone; SVZ, subventricular zone; ISVZ, inner SVZ; OSVZ, outer SVZ; LV, lateral ventricle. Scale bar: 100 and 1000 μm (nuclear staining).

parietal expansion relies on the increase in size of both SVZ compartments.

Next, we examined whether developmental dynamics in the ISVZ and OSVZ differ along the latero-dorsal axis within the same animal. In mice, the ISVZ and OSVZ develop proportionally in the temporal and parietal cortices (Fig. 3*M*,*P*). However in normal ferrets, the parietal ISVZ outgrows the temporal ISVZ during early stages of neurogenesis (from E25 to E33), while the parietal OSVZ outgrows the temporal OSVZ during later stages of neurogenesis (from P0 to P7) (Fig. 3*N*,*Q*). MAM injection at E33 prevents the postnatal expansion of the parietal compared with temporal OSVZ (Fig. 3*O*,*R*). In summary,

overall and regional cortical surface expansion are associated with an increased size of the (1) inner SVZ during early stages of neurogenesis and (2) the outer SVZ during later stages of neurogenesis.

Distribution of Mitotic Cells in the VZ and SVZ

Next, we studied the distribution of actively cycling cells, identified by the expression of PH3, a marker of late G2 and M phases (Hendzel et al. 1997; Scott et al. 2003) (Fig. 4). For comparison of data obtained from normal and E33 MAM-treated ferrets, see Supplementary Figure 7*A–D*.

First, we compared the distribution of PH3+ cells in the mouse and ferret parietal cortex. In mice, the bulk of neurogenesis (i.e. 50% or more PH3+ cells) occurs in the VZ until E17.5 (Figs 4*A* and 5*A*), while in ferrets, it occurs sequentially in the VZ and in the SVZ after E36 (Figs 4*B* and 5*B*). Although the distribution of dividing cells is not altered in P0 MAM-treated ferrets, significant differences are observed a week later with more PH3+ cells in the SVZ (91.66% ±4.16) compared with normal ($P < 0.001$; Figs 4*C* and 5*C*). In the parietal cortex of normal ferrets at P14 (corresponding to the end of neurogenesis (Noctor et al. 1997); 96.21% (±1.93) of PH3+ cells are found in the SVZ (Supplementary Fig. 8*A*,*B*); this is similar to P7 E33 MAM-treated ferrets ($P = 0.378$, *t*-test). This result suggests that MAM exposure results in a premature end to neurogenesis.

In this section, we confirm that the proportion of cycling cells in the SVZ increases throughout mouse and ferret neurogenesis (Martinez-Cerdeno et al. 2006). The shift of dividing cells toward the SVZ occurs earlier in ferrets compared with mice (present study), but also earlier in macaques compared with ferrets (Martinez-Cerdeno et al. 2012). We propose that this "shift" is associated with cortical surface expansion (1) if it occurs prior to the formation of upper cortical layers (E36 for parietal cortex in normal ferrets) and (2) if neurogenesis is protracted as observed in normal ferrets (Martinez-Cerdeno et al. 2006) (but unlike in lissencephalic ferrets).

Next, we compared the distribution of PH3+ cells in the temporal and parietal cortices within the same animal (Figs 4*D–I* and 5*D–I*). In mouse, the "shift" from the VZ toward the SVZ is initiated earlier in the temporal compared with parietal cortex. From E14 to E16, more PH3+ cells are found in the temporal SVZ, while in the parietal cortex, more are found in the VZ ($P = 0.024$ at E14 and $P = 0.033$ at E16) (Fig. 5*D*,*G*), indicating that neurogenesis is more advanced in the temporal cortex. However in normal and lissencephalic ferrets, the temporal and parietal distribution of PH3+ cells are similar (Fig. 5*E–I*). This suggests that, in ferrets, neurogenesis displays a similar degree of advancement in the temporal and parietal cortices. We propose that this characteristic is essential for parietal cortex expansion, but only if neurogenesis is protracted as observed in normal ferrets (Martinez-Cerdeno et al. 2006) but not in E33 MAM-treated ferrets.

In summary, a shift of mitotic cells from the VZ toward the SVZ prior to surpragranular layer formation, associated with protracted neurogenesis, is essential for overall and regional cortical surface expansion.

Dynamics of Mitotic Cell Distribution Within the Inner and Outer SVZ

Does the inner SVZ, the outer SVZ, or both contribute equally to cortical surface expansion? To answer this question, we examined the distribution of dividing cells within the 2 SVZ compartments (Fig. 5*J*,*R* and Supplementary Fig. 7*E–H*).

First, we compared parietal ISVZ and OSVZ and found similar trends in mice and normal ferrets: (1) PH3+ cells are more abundant in the ISVZ (compared with the OSVZ) during most of neurogenesis, in mice until E16 (Fig. 5*J*) and in normal ferrets until P3 (Fig. 5*K*) and (2) PH3+ cells increase constantly in the OSVZ and reach their maximum at the end of neurogenesis. However, the 2 species differ greatly in terms of the PH3+ cell magnitude, particularly in the ISVZ where, in normal ferret, the percentage of PH3+ cells increases at E33 and peaks at P0 (Fig. 5*K*). This is also the case at P0 after MAM treatment, but to a lesser degree compared with normal ($P = 0.041$; Fig. 5*L*). We conclude that an increased percent of PH3+ cells in the ISVZ, when upper cortical layers are being generated, is essential for overall cortical surface expansion.

Next, we examined how PH3+ cells distribute within the inner and outer SVZ along the latero-dorsal axis within the same animal. In mouse, differences between temporal and parietal ISVZ are found from E14 to E16 (higher % of PH3+ cells in the temporal compared with the parietal ISVZ) but not in the OSVZ (Fig. 5*M*,*P*). In normal ferrets, however, the distribution of PH3+ cells is similar in the temporal and parietal ISVZ from E25 to P0, while in the OSVZ, more PH3+ cells are found in the parietal cortex (Fig. 5*N*,*Q*). This suggests that, in normal ferret, (1) neurogenesis in the ISVZ displays a similar degree of advancement in the parietal and temporal cortices, and that (2) neurogenesis in the OSVZ is more advanced in the parietal cortex. Interestingly, after MAM injection, neurogenesis in the ISVZ is more advanced in the temporal cortex but not in the OSVZ, similar to mice (Fig. 5*O*,*R*).

In summary, the results presented in this section demonstrate that (1) an increase in mitotic cells in the ISVZ and OSVZ, prior to the formation of upper cortical layers, is associated with overall and regional cortical surface expansion, and that (2) in ferrets, the ISVZ is the main source of neurons when upper cortical layers are being generated.

Dividing Cell Phenotype in Mouse and Normal Ferret SVZ

The third parameter analyzed is the phenotype of actively cycling cells. We focused on one region, the SVZ, since it plays a major role in overall and regional cortical surface expansion (as demonstrated above). The phenotype of dividing SVZ progenitor cells was analyzed by triple labeling against PH3, Pax6, and Tbr2 (Fig. 6). Pax6 and Tbr2 together detect most cortical progenitor cells (>90%) (Kowalczyk et al. 2009), and the 2 populations found in the SVZ: The oRG and the IP cells. oRG express Pax6 but not Tbr2 (Fietz et al. 2010; Hansen et al. 2010; Reillo et al. 2011), while IP cells express Tbr2 (Englund et al. 2005) and can also co-express Pax6 (Englund et al. 2005; Kowalczyk et al. 2009; Martinez-Cerdeno et al. 2012).

The following results compare the distribution of cycling oRG (i.e. PH3+ cells expressing Pax6, but not Tbr2) and cycling IP cells (i.e. PH3+ cells expressing Tbr2 and Pax6, or Tbr2 alone) in the inner SVZ (Fig. 6*A–K*) and outer SVZ (Fig. 6*L–U*) in mice and normal ferrets.

Inner SVZ

Overall, most dividing cells, in the parietal ISVZ of mice and normal ferrets, are IP cells (Tbr2+Pax6+/−) (Fig. 6*A–D*,*F*,*G*). Differences between mice and ferrets occur during early stages

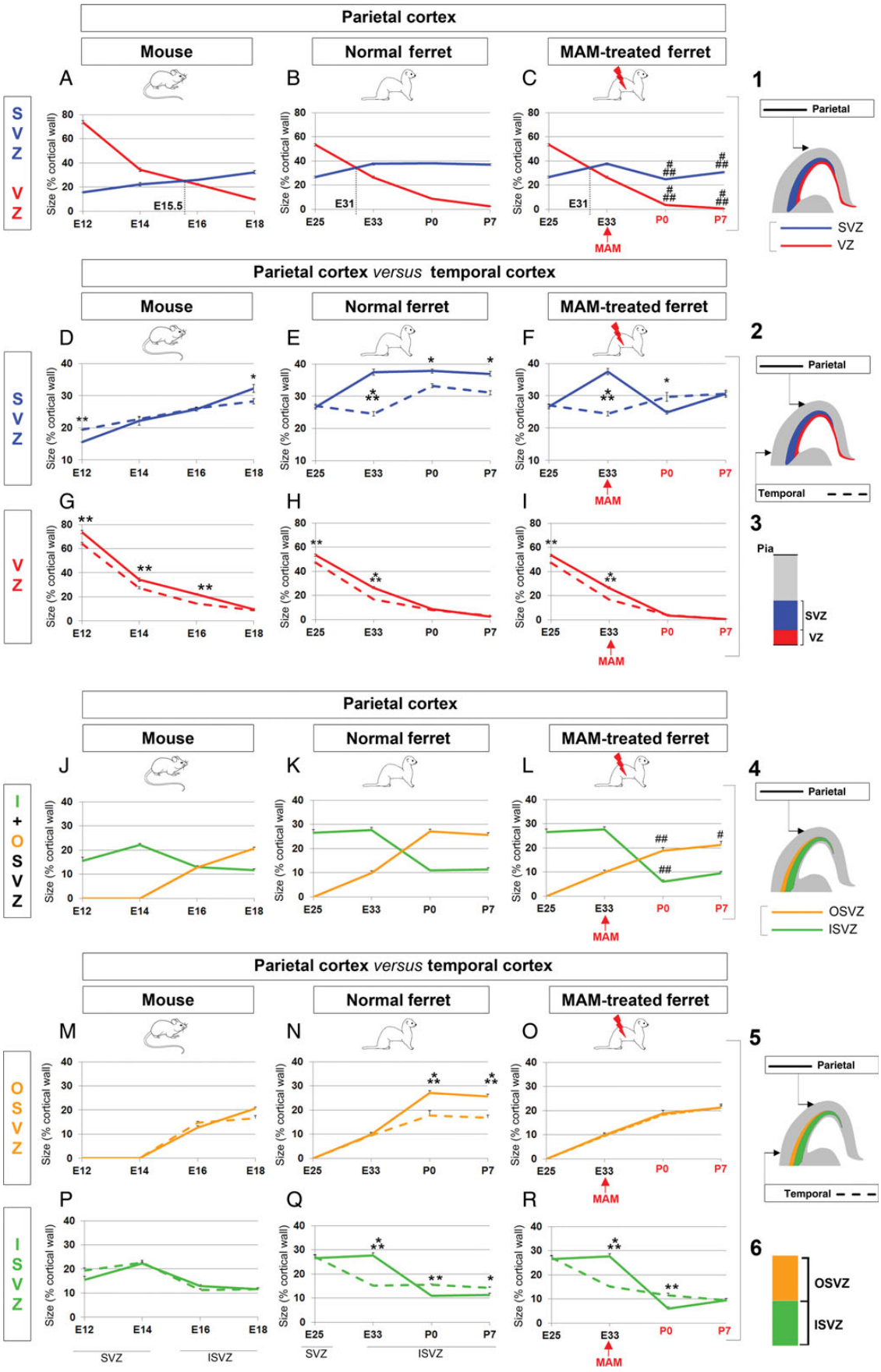
Parietal cortex
Mouse
Normal ferret
MAM-treated ferret
A
B
C
1
S V Z
V Z
Size (% cortical wall)
E15.5
E31
E31
MAM
Parietal
SVZ
VZ
Parietal cortex versus temporal cortex
D
E
F
2
S V Z
Temporal
G
H
I
3
V Z
Pia
SVZ
VZ
Parietal cortex
J
K
L
4
I + O S V Z
OSVZ
ISVZ
Parietal cortex versus temporal cortex
M
N
O
5
O S V Z
Temporal
P
Q
R
6
I S V Z
OSVZ
ISVZ
E12
E14
E16
E18
E25
E33
P0
P7
SVZ
ISVZ

of neurogenesis; indeed in the ferret parietal ISVZ, at E25, 82.22% (±2.18) of PH3+ IP cells express Pax6 compared with only 24.12% (±3.98) at E12 in mice (Fig. 6*F*,*G*). At the end of neurogenesis in both species, few if any dividing Tbr2+Pax6− IP cells are detected (Supplementary Figs 8*C* and 9*C*).

Next, we compared the % of PH3+ IP cells in the temporal and parietal ISVZ within the same species, and no statistical differences were found (Fig. 6*F*,*G*,*I*,*J*). We propose that increase in IP cells expressing Tbr2 and Pax6 in the ISVZ, during early neurogenesis, contributes to the overall cortical surface expansion, but is not essential for regional cortical surface expansion.

Next, we examined the phenotype of dividing oRG in the parietal ISVZ. Although their % increases as neurogenesis progresses, in mice as well as in normal ferrets, PH3+ oRG are observed earlier in ferrets (E33) compared with mice (E16) (Fig. 6*F*,*G*). In addition, oRG onset along the latero-dorsal axis differs in both species. In ferrets starting at E33, similar % of PH3+ oRG are found between temporal and parietal ISVZ, while in mice, more PH3+ oRG are found in the temporal ISVZ at E16 ($P = 0.048$, compared with the parietal ISVZ) (Fig. 6*F*,*G*, *I*,*J*). We propose that overall and regional cortical surface expansion in ferrets rely on the premature onset of dividing oRG cells in the ISVZ compared with mice.

Outer SVZ

Similar to the ISVZ, differences between mouse and ferret OSVZ occur during early stages of neurogenesis as most (>70%) cycling cells are IP cells in the mouse and oRG cells in the ferret (Fig. 6*P*,*Q*). In both species, toward the end and after completion of neurogenesis, most PH3+ cells (>60%) are oRG (Supplementary Figs 8*C* and 9*C*). Next, we compared the phenotype of dividing OSVZ progenitor cells in the temporal and parietal cortices within the same species and found no difference (Fig. 6*P*,*Q*,*S*,*T*). In conclusion, we propose that early onset of oRG in the ferret OSVZ contributes to overall and regional cortical expansion.

Dividing Cell Phenotype in the SVZ After MAM Exposure

In E33 MAM-treated ferrets, the reduction (compared with normal) of dividing IP cell %, in the ISVZ and OSVZ, suggests that MAM exposure results in a premature end to neurogenesis (Fig. 6*H*,*K*,*R*,*U*). To test this hypothesis, Tbr2 and Pax6 expression levels were evaluated by western blot analysis. We also tested whether BLBP expression level is altered since this radial marker is downregulated in radial glial cells starting at P3 in normal ferrets (Poluch and Juliano 2010). Compared with normal, newborn E33 MAM-treated kits show a reduction in Tbr2 and BLBP expression levels ($P = 0.003$ and 0.004, respectively, Supplementary Fig. 10*A*,*C*) and also a reduction in BLBP expression in radial glial cells (Supplementary Fig. 10*D*–*G*). Radial glial morphology is not disrupted after MAM exposure at E33, unlike at E24 (Noctor et al. 1999; Hasling et al. 2003; Poluch and Juliano 2010). In contrast to Tbr2 and BLBP, Pax6 expression was unchanged after MAM treatment (Supplementary Fig. 10*B*); this result is not surprising since oRG, unlike radial glia, persist after neurogenesis and are thought to participate in gliogenesis (Martinez-Cerdeno et al. 2012). In conclusion, changes in progenitor cell phenotype observed in lissencephalic ferrets (i.e. less IP cells and more oRG compared with normal) are likely the result of premature end of neurogenesis and early onset of gliogenesis.

Dividing Cell Phenotype in the VZ + ISVZ Versus OSVZ

In human, comparison of progenitor cell types and proportions demonstrates that the OSVZ is a duplicated VZ/ISVZ (Hansen et al. 2010). To assess whether this characteristic is specific to gyrencephalic brains, or observed as well in lissencephalic brains, the phenotype of OSVZ progenitor cells was compared with VZ/ISVZ progenitor cells in the parietal cortex of mice, normal, and lissencephalic ferrets (Fig. 7 and Supplementary Table 1).

During neurogenesis, cycling progenitor cell types in the VZ/ISVZ and OSVZ are different in mice (from E16 to E18; Fig. 7*A*,*B*) and in lissencephalic ferrets (from P0 to P7; Fig. 7*F*, *G*), but similar in normal ferrets (from E33 to P0; Fig. 7*C*,*D*). After completion of neurogenesis (P0 in mice and P14 in normal ferrets), VZ/ISVZ and OSVZ contain similar progenitor cell types (Supplementary Figs 8*C* and 9*C*). In conclusion, duplication of the VZ/ISVZ into the OSVZ occurs (1) in normal ferrets, during early stages of neurogenesis, (2) in mice, during early stages of gliogenesis, (3) but fails in ferrets after MAM exposure. This result suggests that the timing of VZ/ISVZ duplication is fundamental; duplication prior to surpragranular layer formation is a characteristic found only in gyrencephalic brain species.

Discussion

The present study provides new insights into mechanisms underlying overall and regional cortical surface expansion by demonstrating that they both rely on changes in timing rather than the sequence of neurogenic events. We propose that onset of oRG and increase in IP cells expressing Pax6, prior to surpragranular layer formation, are essential for expansion of the SVZ and a gyrencephalic cortex. We also propose that

Figure 3. Proliferating zone size evolution during neurogenesis in mouse, normal ferrets and lissencephalic ferrets. (*A*–*I*) VZ versus SVZ. Comparison in the parietal cortex of mouse (*A*), normal ferrets (*B*), and E33 MAM-treated ferrets (*C*). The VZ is shown in red and the SVZ in blue (see illustrations 1 and 3). The black dotted lines (on graphs *A*–*C*) indicate an extrapolated developmental stage at which the size of the VZ equals that of the SVZ. Comparison between temporal and parietal cortices in mouse (*D* and *G*), normal ferrets (*E* and *H*), and E33 MAM-treated ferrets (*F* and *I*). As indicated in 2, data obtained in the parietal cortex are illustrated with a plain line (red for VZ and blue for SVZ) and those obtained in the temporal cortex are illustrated with a dashed line (red for VZ and blue for SVZ). (*J*–*R*) Inner SVZ versus outer SVZ. Comparison in the parietal cortex of mouse (*J*), normal ferrets (*K*), and E33 MAM-treated ferrets (*L*). The inner SVZ is shown in green and the outer SVZ in orange (see illustrations 4 and 6). Comparison between temporal and parietal cortices in mouse (*M* and *P*), normal ferrets (*N* and *Q*), and E33 MAM-treated ferrets (*O* and *R*). As indicated in 5, data obtained in the parietal cortex are illustrated with a plain line (green for inner SVZ and orange for outer SVZ) and those obtained in the temporal cortex are illustrated with a dashed line (green for inner SVZ and orange for outer SVZ). Data presented in graphs are expressed as a percentage of the cortical thickness. Statistical analysis: 3 animals for each developmental stage; for each animal, results are averaged from 2 slices. $^{\#\#\#}P < 0.001$, $^{\#\#}P < 0.003$, $^{\#}P = 0.028$ (normal ferrets compared with E33 MAM-treated ferrets; *B* vs. *C* and *K* vs. *L*); $^{***}P < 0.001$, $^{**}P = 0.002$, $^{*}0.028 < P < 0.044$ (parietal cortex compared with temporal cortex); *t*-test. The red arrows indicate the time of MAM injection (E33); developmental stages (P0 and P7) in red indicate that cortical development is affected by MAM exposure; developmental stages in black indicate that cortical development is normal (without MAM exposure or prior to MAM exposure). VZ, ventricular zone; SVZ, subventricular zone; ISVZ, inner SVZ; OSVZ, outer SVZ.

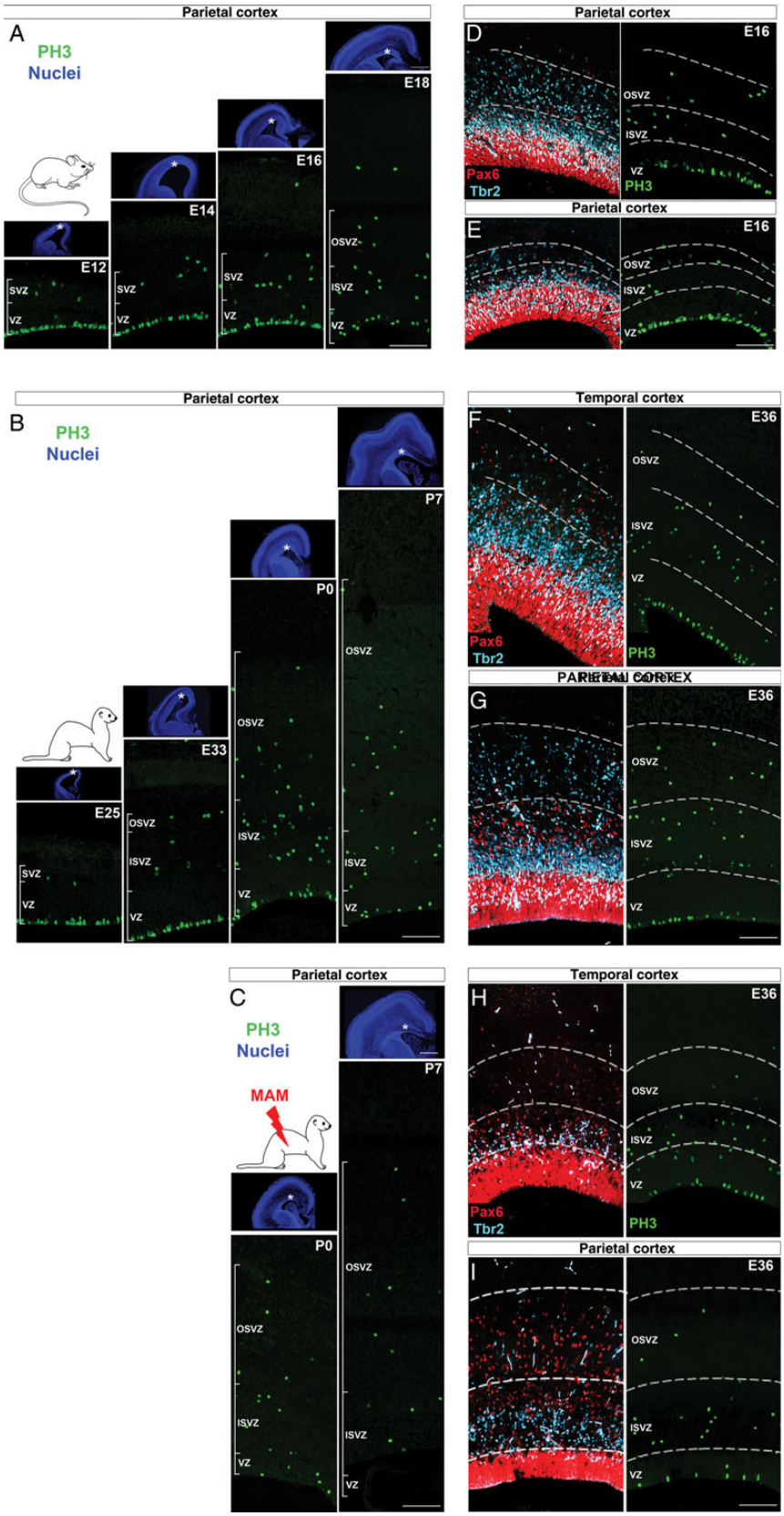

Figure 4. Localization of mitotic cells during neurogenesis. Immunostaining against PH3 (green) followed by nuclear counterstaining (blue) in the parietal cortex of mouse embryos from E12 to E18 (*A*), normal ferrets from E25 to P7 (*B*), and E33 MAM-treated ferrets from P0 to P7 (*C*). Asterisks on low-magnification pictures (nuclear staining) indicate the localization of proliferating regions in the parietal cortex. Immunostaining against PH3 (green), Pax6 (red), and Tbr2 (cyan) in the temporal and parietal cortices at E16 in mouse (*D* and *E*), at E36 in normal ferrets (*F* and *G*), and E36 in E33 MAM-treated ferrets (*H* and *I*). Scale bar: 500 μm (PH3) and 100 μm (nuclear staining). VZ, ventricular zone; SVZ, subventricular zone; ISVZ, inner SVZ; OSVZ, outer SVZ.

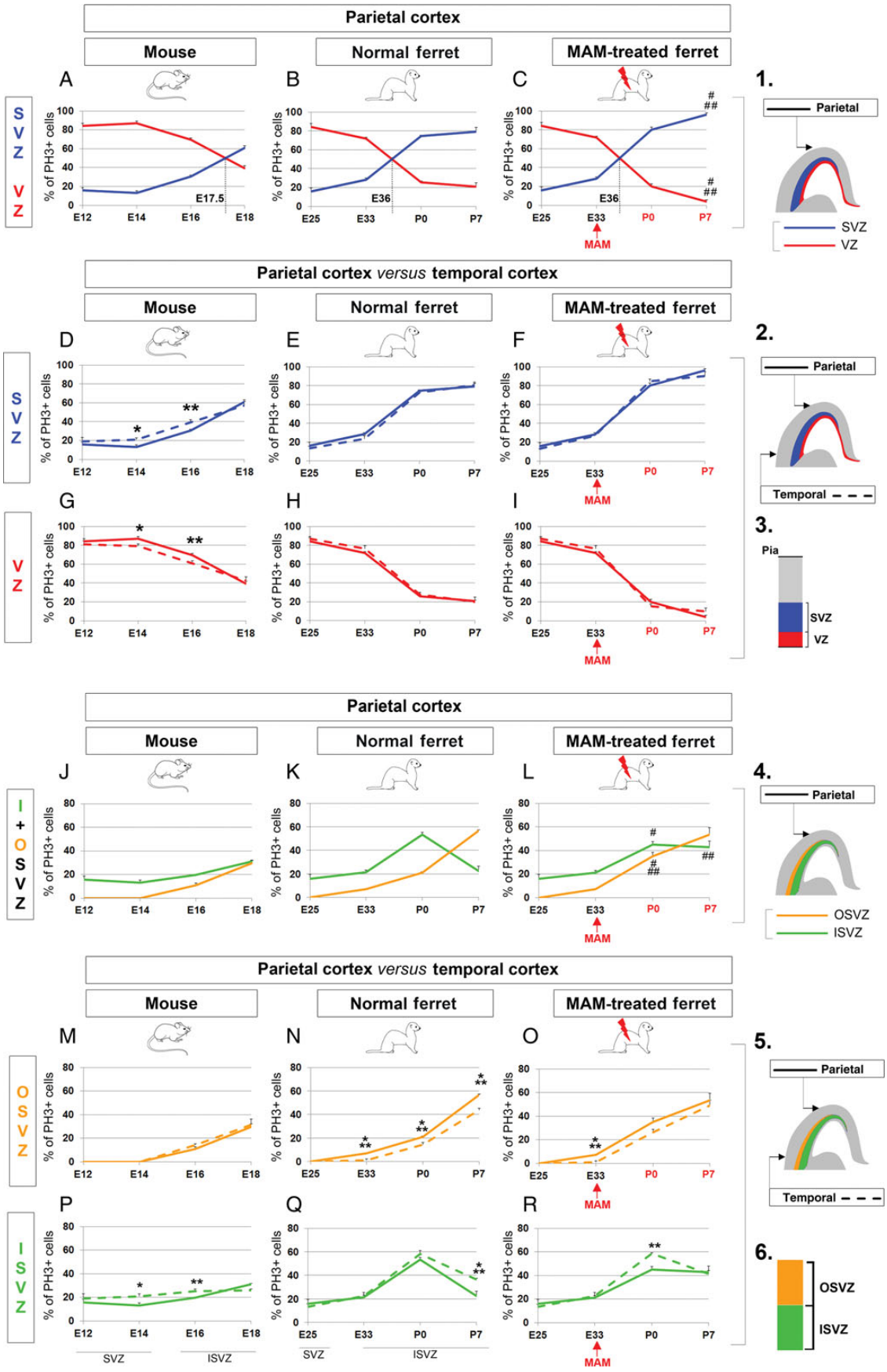
Parietal cortex
Mouse
Normal ferret
MAM-treated ferret
A
B
C
SVZ
VZ
% of PH3+ cells
E17.5
E36
E36
E12
E14
E16
E18
E25
E33
P0
P7
MAM
1.
Parietal
SVZ
VZ
Parietal cortex versus temporal cortex
D
E
F
G
H
I
2.
Temporal
3.
Pia
I+OSVZ
Parietal cortex
J
K
L
4.
OSVZ
ISVZ
Parietal cortex versus temporal cortex
M
N
O
P
Q
R
5.
6.
SVZ
ISVZ

regional cortical surface expansion is achieved by altering the latero-dorsal gradient of neurogenesis.

How to Build a Bigger Brain: Insights From Comparative Studies Between Different Species

Protracted neurogenesis is essential for evolutionary expansion of the neocortical surface (Rakic 1988, 1995). This is achieved by changes in cell cycle kinetics that delay the switch from symmetrical to asymmetrical divisions (reviewed in Dehay and Kennedy 2007). As a result, production of neurons is protracted and the pool of cortical progenitor cells is amplified. The region that expands the most, in terms of size and progenitor cell number, is the SVZ; particularly the outer portion in primates and the inner portion in carnivores, including ferrets (Smart et al. 2002; Lukaszewicz et al. 2005; Martinez-Cerdeno et al. 2006, 2012; Hansen et al. 2010; Reillo et al. 2011). In this study, we demonstrate differences in the course of neurogenesis between lissencephalic and gyrencephalic brains that provide a basis for the evolutionary expansion of ferret inner SVZ and possibly human outer SVZ.

First, dividing oRG are detected in ferret ISVZ during early phases of neurogenesis (prior to supragranular layer formation), while they are detected in mouse ISVZ during later stages (when surpragranular layers are being formed). Because oRG were first identified in the OSVZ (Fietz et al. 2010; Hansen et al. 2010) and ISVZ (Reillo et al. 2011) of folded-brain species, they were thought to be essential to cortical surface expansion. Their detection later in smooth brain species challenged this hypothesis (Shitamukai et al. 2011; Wang et al. 2011; Garcia-Moreno et al. 2012; Kelava et al. 2012; Martinez-Cerdeno et al. 2012). Based on our observations, we propose that oRG are essential for gyrification if their onset occurs during early stages of neurogenesis so they can participate, in addition to radial glia (RG) and IP cells, in the expansion of the cortical progenitor cell pool. This is consistent with observations that the oRG population reaches 50% of all cortical progenitor cells in humans and ferrets (Fietz et al. 2010; Hansen et al. 2010; Reillo et al. 2011) and only 10% in mice (Shitamukai et al. 2011; Wang et al. 2011). The somewhat late detection of dividing oRG in mouse ISVZ suggests that their contribution to neurogenesis is minor compared with ferrets. Finally, if oRG are essential for gyrification as we propose, why is the percentage of dividing oRG increased in E33 MAM-treated kits compared with normal? This observation does not necessarily refute our hypothesis since at least 2 oRG subpopulations coexist in the SVZ: oRG that do not express Olig2 are presumably neurogenic progenitor cells, while those expressing Olig2 are presumably gliogenic progenitor cells (Martinez-Cerdeno et al. 2012). Newborn lissencephalic ferrets display a reduction in the number of cycling IP cells, in the level of Tbr2 and BLBP expression, and in radial glial density. Because these changes suggest that MAM treatment induces an early end of neurogenesis, we propose that cycling oRG in E33 MAM-treated ISVZ are involved in gliogenesis rather than in neurogenesis.

The second significant difference between mouse and ferret ISVZ is the phenotype of dividing IP cells. Prior to supragranular layer formation in ferrets, the majority of IP cells co-express Pax6 and Tbr2. Similar results are found in mice, but during late stages of neurogenesis, as well as in ferrets after MAM exposure. Expression of Pax6 in IP cells has been reported previously in different species and at different stages of development (Englund et al. 2005; Kowalczyk et al. 2009; Fietz et al. 2010; Hansen et al. 2010; Martinez-Cerdeno et al. 2012). Pax6+ IP cells are thought to be newly generated or undifferentiated as opposed to differentiated IP cells expressing low-to-absent levels of Pax6 (Kowalczyk et al. 2009). IP cells have the capacity to undergo 1 or 2 subsequent symmetric divisions prior to asymmetric division and the production of a postmitotic neuron (Haubensak et al. 2004; Miyata et al. 2004; Noctor et al. 2004, 2008). Based on our results, one can speculate that Pax6 expression in ferret IP cells during early neurogenesis promotes symmetric proliferative division rather than symmetric terminal division and, therefore, amplification of the IP cell pool. The fact that, at the end of neurogenesis (in mice as well as in normal ferrets) or after MAM exposure, most IP cells express that Pax6 does not contradict this hypothesis. Indeed, several studies reveal dual functions of the gene *Pax6*. Among those, Holm et al. (2007) describe, using microarray analysis in Pax6-mutant mice *Small Eye* ($Pax6^{Sey}-/-$), a decreased expression of *Tbr2* at E12 and thatof growth arrest genes at E15. These results support our hypothesis that Pax6 expression in IP cells participates in different processes during early and late neurogenesis.

In conclusion, we propose that the early onset of oRG and the increased percentage of Pax6+ IP cells contribute to ferret gyrification; however, the contribution of oRG and IP cells is more likely complementary. Only a low percentage of ferret oRG are neurogenic (<5% express Tbr2; Fietz et al. 2010; Reillo et al. 2011; Reillo and Borrell 2012); they initially produce more oRG by self-amplification and later produce astrocytes (Reillo et al. 2011; Martinez-Cerdeno et al. 2012). Although these studies suggest that the contribution to neurogenesis from oRG cells is minor compared with IP cells in ferret, others show that oRG are essential to gyrification as they provide additional guides to the

Figure 5. Mitotic cell distribution during neurogenesis in mouse, normal ferrets and lissencephalic ferrets. (*A–I*) VZ versus SVZ. Comparison in the parietal cortex of mouse (*A*), normal ferrets (*B*), and E33 MAM-treated ferrets (*C*). The VZ is shown in red and the SVZ in blue (see illustrations 1 and 3). The black dotted lines (on graphs *A–C*) indicate an extrapolated developmental stage at which the % of PH3+ cells in the VZ equals the % of PH3+ cells in the SVZ. Comparison between temporal and parietal cortices in mouse (*D* and *G*), normal ferrets (*E* and *H*), and E33 MAM-treated ferrets (*F* and *I*). As indicated in 2, data obtained in the parietal cortex are illustrated with a plain line (red for VZ and blue for SVZ) and those obtained in the temporal cortex are illustrated with a dashed line (red for VZ and blue for SVZ). (*J–R*) Inner SVZ versus outer SVZ. Comparison in the parietal cortex of mouse (*J*), normal ferrets (*K*), and E33 MAM-treated ferrets (*L*). The inner SVZ is shown in green and the outer SVZ in orange (see illustrations 4 and 6). Comparison between temporal and parietal cortices in mouse (*M* and *P*), normal ferrets (*N* and *Q*), and E33 MAM-treated ferrets (*O* and *R*). As indicated in 5, data obtained in the parietal cortex are illustrated with a plain line (green for inner SVZ and orange for outer SVZ) and those obtained in the temporal cortex are illustrated with a dashed line (green for inner SVZ and orange for outer SVZ). Data presented in graphs are expressed as a percentage of PH3+ cells. Statistical analysis: 3 animals for each developmental stage; for each animal, results are averaged from 2 slices. $^{\#\#\#}P < 0.001$, $^{\#\#}P = 0.010$, $^{\#}P = 0.041$ (normal ferrets compared with E33 MAM-treated ferrets; *B* vs. *C* and *K* vs. *L*); $^{***}P < 0.001$, $^{**}P = 0.011$, $^{*}0.022 < P < 0.024$ (SI cortex compared with temporal cortex); *t*-test. The red arrows indicate the time of MAM injection (E33); developmental stages (P0 and P7) in red indicate that cortical development is affected by MAM exposure; developmental stages in black indicate that cortical development is normal (without MAM exposure or prior to MAM exposure). VZ, ventricular zone; SVZ, subventricular zone; ISVZ, inner SVZ; OSVZ, outer SVZ.

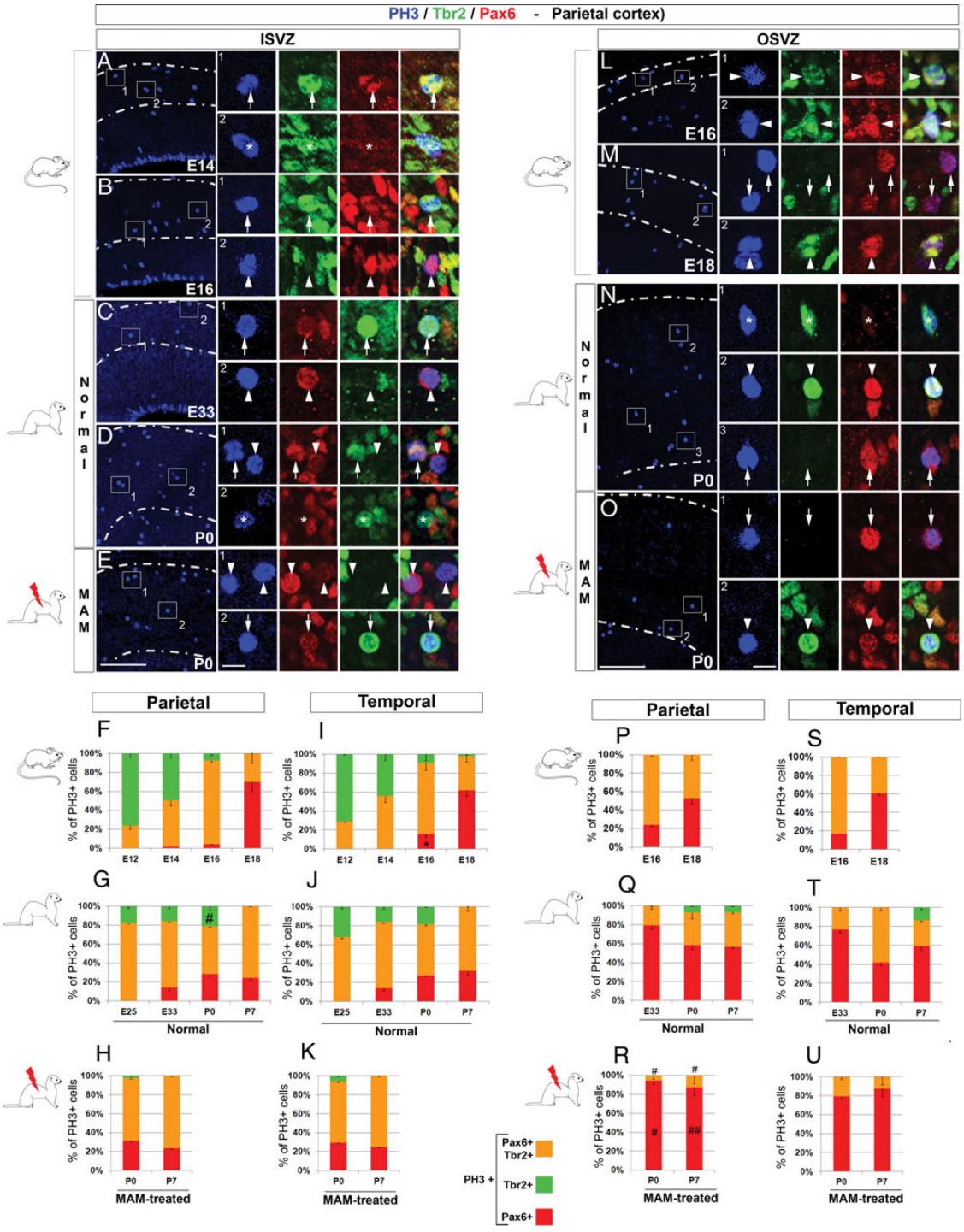

Figure 6. Inner and outer SVZ mitotic cell phenotype in mouse, normal ferrets and lissencephalic ferrets. Immunostaining against PH3 (blue), Tbr2 (green), and Pax6 (red). Pictures in on the left panel show the parietal ISVZ (*A–E*) and pictures on the right panel show the parietal OSVZ (*L–O*). Higher magnifications are from the boxed area (1 and 2); arrows indicate PH3+Pax6+ cells, arrow heads PH3+Tbr2+Pax6+ cells, and asterisks PH3+Tbr2+ cells. Graphs represent the % of PH3+ cells expressing Pax6+ (red), Tbr2+ (green), or Pax6+ and Tbr2+ (orange) in the parietal ISVZ (*F–H*), temporal ISVZ (*I–K*), parietal OSVZ (*P–R*), and temporal OSVZ (*S–U*). Note that the inner and outer SVZ are discernable in mouse starting at E16 and E33 in ferrets; data presented prior to E16 and E33 are from the SVZ. Statistical analysis: 3 animals for each developmental stage; for each animal, results are averaged from 2 slices. The total number of PH3+ cells analyzed in the ISVZ ranges from 48 to 63 in mice, 59 to 266 in normal ferrets, and 28 to 107 in E33 MAM-treated ferrets; the total number of PH3+ cells analyzed in the OSVZ ranges from 37 to 52 in mice, 42 to 102 in normal ferrets, and 23 to 53 in E33 MAM-treated ferrets. $^{\#}0.032 < P < 0.018$ (normal ferrets compared with E33 MAM-treated ferrets; *G* vs. *H* and *Q* vs. *R*); $^{*}P = 0.010$ (parietal cortex compared with temporal cortex); *t*-test. Scale bar: 100 μm (*A–E* and *L–O*) and 10 μm (higher magnification).

increased number of neurons produced in gyrencephalic species (Smart et al. 2002; Reillo et al. 2011; Stahl et al. 2013). Human oRG appear different from those in ferrets, although their morphology is similar, they are neurogenic and contribute to increasing the pool of progenitor cells (Hansen et al. 2010).

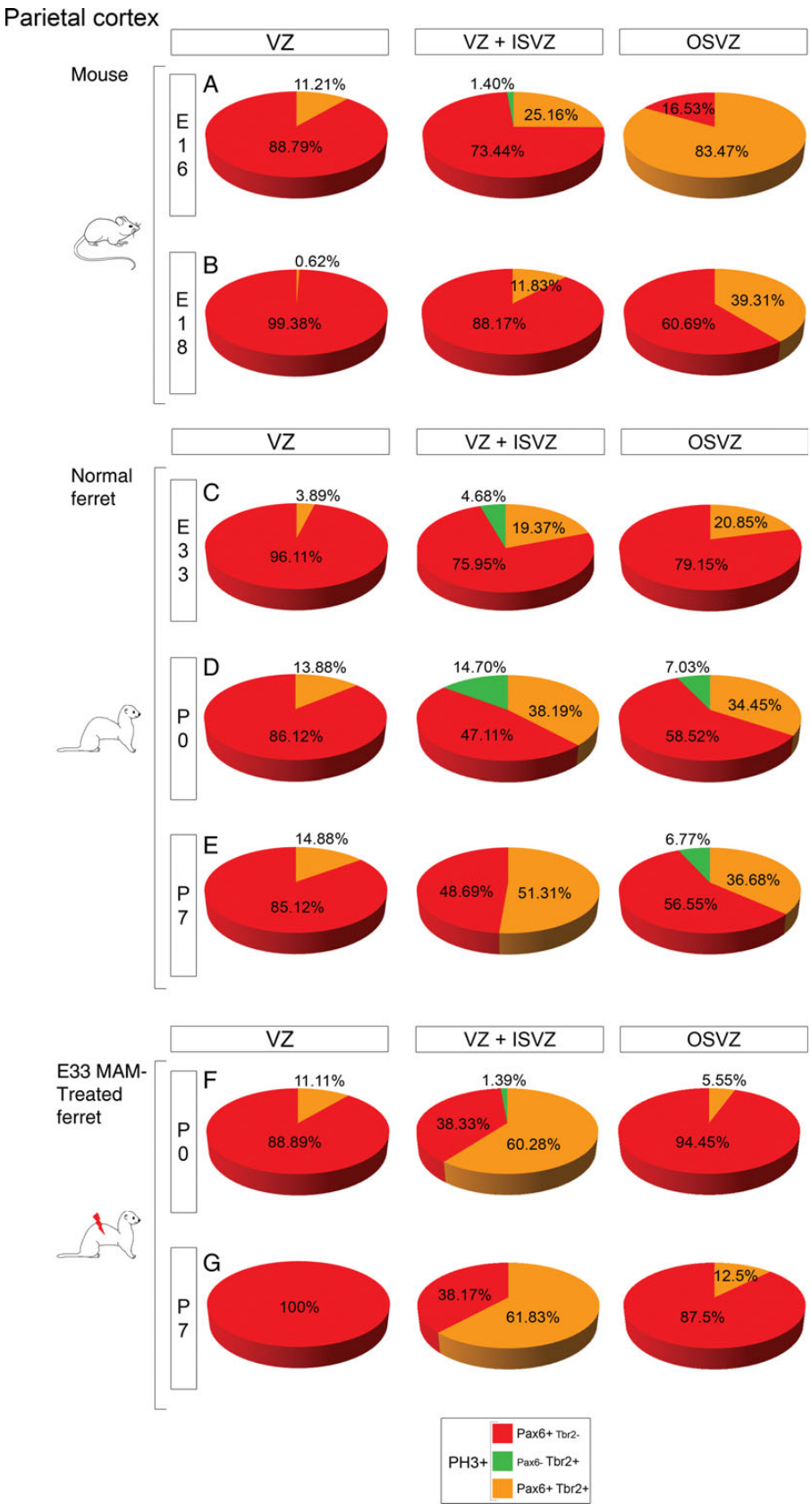

Figure 7. Phenotype of dividing cells in the parietal VZ, VZ + ISVZ, and OSVZ. Pies represent the phenotype of PH3+ cells in the VZ (left panel), VZ + ISVZ (middle panel), and OSVZ (right panel) in mouse at E16 and E18 (*A* and *B*), normal ferrets at E33, P0, and P7 (*C*–*E*), and in E33 MAM-treated ferrets at P0 and P7 (*F* and *G*). Analysis was performed at developmental stages showing compartmentalization of the SVZ into an inner and outer compartment. Three animals for each developmental stage; for each animal, results are averaged from 2 slices. Two-way ANOVA was conducted followed by a Holm-Sidak test for comparisons between groups; *P*-values are presented in Supplementary Table 1.

How to Achieve Regional Cortical Surface Expansion: Insights From Comparative Studies Between Different Cortical Regions Within the Same Animal

Neurogenesis in gyrencephalic brains is not homogenous as particular regions differ in the number of neurons they produce (Dehay et al. 1993; Lukaszewicz et al. 2006; Reillo et al. 2011). Experiments in the primate visual cortex show that changes in cell cycle kinetics are essential in this process (Dehay et al. 1993; Kornack and Rakic 1998; Lukaszewicz et al. 2005, 2006). In the present report, we compared the dynamics of neurogenic events in 2 cortical regions of normal ferrets presenting differences in neuron production (the more enlarged parietal surface compared with the temporal surface). Our goal was to reveal mechanisms involved in regional cortical surface expansion. We also used mice and E33 MAM-treated ferrets as a comparison; although the former is lissencephalic and the latter moderately lissencephalic, in both, parietal and temporal cortices expand to similar degree. Here, we demonstrate that, in normal ferrets, parietal expansion (compared with temporal) is associated with early SVZ growth and oRG onset. Although IP cells display a similar phenotype in both regions, we cannot exclude that variations in cell cycle kinetics contribute to parietal SVZ expansion. Finally, distribution of cycling cells is similar between parietal and temporal regions, unlike in mice and in lissencephalic ferrets. Altogether, our results suggest that ferret parietal expansion relies on an early onset of neurogenesis.

Our findings do not contradict the well-established latero-dorsal gradient of cortical development. Seminal studies in mammals, including mice and ferrets, examined the size of the cortical plate or the distribution of (^{3}H)-thymidine neurons, and concluded that more neurons are produced laterally than dorsally (Smart and Smart 1977; McSherry 1984; McSherry and Smart 1986). Here, we demonstrate that neurogenesis in mice follows a similar gradient (i.e. latero-dorsal gradient of neurogenesis), as neurogenic events are more advanced in the temporal region. In ferrets, however, there is a discrepancy between the gradient of cortical development and neurogenesis. Indeed, if the temporal region is more mature in terms of neuron production (McSherry 1984; McSherry and Smart 1986), neurogenesis displays similar degree of progression in the temporal and parietal regions. This suggests that elimination of the latero-dorsal gradient of neurogenesis is a prerequisite for greater expansion of the parietal cortex. Accordingly, the duration of the phase consisting in expansion of the founder cell pool is increased, and more neurons are produced (Rakic 1988). The finding that the lateral–dorsal gradient of neurogenesis is reestablished after MAM exposure (as in mice) strongly supports our hypothesis.

What are the factors that could alter the timing of parietal neurogenesis and ultimately the gradient of neurogenesis? Secreted morphogens are good candidates as they control graded expression of transcription factors, such as Pax6, essential for cortical regional patterning, including the rostro-caudal and dorso-ventral axes, neurogenesis (reviewed in Caviness et al. 2009), and brain morphogenesis (Dahmane and Ruiz i Altaba 1999). For example, overexpression of FGF2 increases cortical volume in rats and induces gyrification in mice (Vaccarino et al. 1999; Rash et al. 2013), while decreased proliferation is observed in the VZ and SVZ of sonic hedgehog null embryos (Dahmane et al. 2001). Therefore, inhibition or de novo expression of a morphogen could increase the proliferation rate in the ferret parietal cortex. This hypothesis is conceivable based on recent findings by Charrier et al. (2012) as they demonstrate that changes in the expression of a single gene (i.e. SRGAP2) had a profound impact on human brain evolution. Finally, the finding that the rostro-caudal gradient of Pax6 expression, initially described in mice, disappears during early corticogenesis in human (Bayatti et al. 2008; Ip et al. 2010) suggests that the spatio-temporal expression of morphogens might differ in convoluted brain species.

In addition to a genetic control, as defined by the protomap model (Rakic 1988), neurogenesis is influenced by extrinsic signals (protocortex or *tabula rasa* model) (Van der Loos and Woolsey 1973; O'Leary 1989). These environmental signals, influencing fate and proliferation rates (McConnell and Kaznowski 1991; Dehay et al. 2001; Polleux et al. 2001), may be provided largely by thalamocortical axons (Dehay et al. 2001). In primates, binocular enucleation results in size reduction of the primary visual cortex (Rakic 1988; Dehay et al. 1989). Similar experiments in ferrets show a decrease in IP cells in the outer SVZ (Reillo et al. 2011). Because MAM exposure at E33 alters the distribution of thalamic afferents in the parietal cortex (Noctor et al. 2001; Palmer et al. 2001), one might speculate that aberrant thalamic inputs contribute to the lissencephalic phenotype in E33 MAM-treated ferrets.

Further studies are needed to identify intrinsic and extrinsic signals controlling regional cortical surface expansion. Understanding the underlying mechanisms are important to human disease as specific regions present reduced or increased cortical folding in schizophrenia and autism (Kulynych et al. 1997; Hardan et al. 2004).

Inner and Outer SVZ Contribution to Neurogenesis and Evolution of the Cerebral Cortex

Birth dating studies (Smart et al. 2002; Lukaszewicz et al. 2005; Dehay and Kennedy 2007) and characterization of transcription factor expression (Tarabykin et al. 2001; Nieto et al. 2004; Zimmer et al. 2004) suggest that neurons produced in the SVZ are destined to layers II/III. Although conflicting studies have been published (Haubensak et al. 2004; Sessa et al. 2008; Kowalczyk et al. 2009), this concept provides a convincing explanation to gross anatomical features observed in folded brains such as expansion of upper cortical layers (compared with lower cortical layers) (DeFelipe et al. 2002) and an enlarged SVZ (Smart et al. 2002; Zecevic et al. 2005; Martinez-Cerdeno et al. 2006). In primates, the outer component of the SVZ shows a substantial increase in size and in progenitor cell density, prior to and during formation of upper layer neurons (Smart et al. 2002; Lukaszewicz et al. 2005; Hansen et al 2010; Martinez-Cerdeno et al. 2012). We show that, in normal ferrets, the inner SVZ expands prior to, and the outer SVZ during, upper cortical layer formation; however, the inner SVZ remains the major source of neurons as indicated by the higher percentage of cycling cells. Our results, combined with others cited above, suggest a correlation between the degree of cortical folding and the primary source of neurons prior to and during formation of layers II/III: Lissencephalic brains (VZ), low-to-moderate folded brains (ISVZ), and highly folded brains (OSVZ). This gradual and modular expansion of proliferating regions agrees with the model proposed by Charvet and Striedter (2011). This model states that when the pool of

VZ progenitor cells increases faster than the VZ can expand, progenitor cells leave the VZ and proliferate to form the SVZ. We propose that similar mechanisms contribute to the formation of the inner and outer SVZ. Accordingly, when the cell density in the SVZ reaches its maximum, progenitor cells (possibly from the VZ and/or the SVZ itself) proliferate above the SVZ forming an outer SVZ and an inner SVZ (former SVZ). Based on this gradual construction, building a brain larger than a ferret brain, would rely on expanding the outer SVZ. This is consistent with findings obtained in humans (Hansen et al. 2010), nonhuman primates (Smart et al. 2002; Martinez-Cerdeno et al. 2012), and in normal ferrets as we show that the region expanding the most (i.e. parietal cortex) contains more mitotic figures in the outer SVZ, but not in the inner SVZ (compared with temporal). However, our results differ from those obtained by Reillo et al. (2011) as they show, in cats and humans, an increased density in cycling cells in both the inner and outer parietal SVZ compared with temporal. These dissimilarities could be due to several factors, including differences in the methodology used to delineate the boundaries between proliferation zones. They could also explain why we found that the ferret inner and outer SVZ contain different progenitor cell classes (more IP cells and more oRG, respectively), while others found a similar composition (Reillo et al. 2011, Reillo and Borrell 2012). In fact, our results are similar to humans and suggest, as proposed by Hansen et al. (2010), that the OSVZ is a duplicated VZ/ISVZ. In addition, we show that the duplication occurs during early stages of ferret neurogenesis, prior to surpragranular formation, and also in mice but after completion of neurogenesis. Compartmentalization of SVZ into an inner and outer component is not specific to species with convoluted brains (Garcia-Moreno et al. 2012; Kelava et al. 2012; Martinez-Cerdeno et al. 2012). We reach similar conclusions regarding VZ/ISVZ duplication in the OSVZ; here again, our findings point in the direction of changes in developmental timing between folded and nonfolded brains rather than evolutionary novelty specific to folded brains. In conclusion, we propose that the outer SVZ produces a gyrencephalic cortex only if it expands prior to the onset of upper cortical layers and if it is a duplicated VZ/ISVZ. This hypothesis could be tested by analyzing lissencephalic primates or gyrencephalic rodents similar to Garcia-Moreno et al. (2012) and Kelava et al. (2012).

How Does MAM Affect Ferret Cortical Expansion?

MAM is a methylating agent that targets dividing neuronal progenitors, while postmitotic neurons and glial cells are not affected (Johnston and Coyle 1979; Cattaneo et al. 1995). Because MAM is mainly used to produce models of neuronal migration disorders, epilepsy, or schizophrenia (Germano and Sperber 1998; Hasling et al. 2003; Penschuck et al. 2003), little is known about the effects of MAM on cortical progenitor cells. Nevertheless, based on our results, we can speculate that the following 3 mechanisms participate in decreasing cortical surface expansion in E33 MAM-treated ferrets. (1) First, increased cell death. MAM induces apoptosis in the cerebellar granule cell layer via activation of caspase 3 (Ferrer et al. 2001). The opposite (i.e. reduction of apoptosis) produces gyrification in mice as demonstrated by mutations of death-effector gene families, including Jnk1/2 and caspase 9 (Kuida et al. 1998; Haydar et al. 1999). (2) Secondly, increased cell cycle exit. This hypothesis is consistent with our findings that E24 and E33 MAM-treated ferrets undergo a premature end to neurogenesis (Noctor et al. 1999; present study). Controlling the balance between cell cycle exit and cell cycle reentry is critical for progenitor cell expansion. Genetic mutations in mice show that overexpression of $p27^{Kip1}$ increases cell cycle exit and results in a thinner cortex (Tarui et al. 2005), whereas expression of a stabilized β-catenin associates with a larger brain and formation of sulci due to a greater number of precursor cells undergoing additional rounds of mitosis (Chenn and Walsh 2002, 2003). (3) Thirdly, changes in cell cycle duration. In mice, reduction of G1 duration via forced expression of cyclin D1 and cyclin E1 expands the pool of precursor cells by promoting self-renewing proliferative divisions of radial glia and IP cells (Pilaz et al. 2009). Van den Berg and Ball (1972) demonstrated that Hela cells exposed to MAM show delay in subsequent interphase and S phase. It needs to be determined whether MAM affects G1 duration of cortical precursor cells in E33 MAM-treated ferrets.

E33 MAM-Treated Ferrets as an Animal Model of Lissencephaly

In human, lissencephaly is a rare malformation characterized by simplified cortical gyration pattern and usually associated with a normal sized head at birth. Classically, this brain malformation is described as a neuronal migration disorder (reviewed by Kerjan and Gleeson 2007). However, the radial unit model proposed by Rakic (1988) predicts that lissencephaly can also result from disruption of early phases of neurogenesis. This hypothesis is reinforced by the findings that candidate genes for lissencephaly encode proteins controlling neuronal migration and cell division (Yingling et al. 2008; Pramparo et al. 2010). The different animal models of lissencephaly developed (mainly mice and rats) are interesting to study in relation to the neuronal migration defects associated with the disease, but are limited in exploring the neurogenic component due to the lack of gyration in the rodent cortex. E33 MAM-treated ferrets, however, present defects in neurogenesis leading to reduced cortical surface as presented here and also defects in neuronal migration (Poluch et al. 2008; Abbah and Juliano 2013). In conclusion, E33 MAM-treated ferrets are a unique and valuable model to understand the evolutionary expansion of the cerebral cortex and human lissencephaly.

Supplementary Material

Supplementary material can be found at: http://www.cercor.oxfordjournals.org/.

Funding

This work was supported by the Uniformed Services University/Department of Defense (R0705E and R0702005 to S.P.) and the National Institute of Neurological Disorders and Stroke (NS 24014 to S.L.J.).

Notes

We thank Mireille Rossel, Martin Doughty, and Steve Noctor for helpful comments and critically reading the manuscript; and Mitali Chatterjee and LaToya Hyson for excellent care of the ferrets. The anti-Pax6 monoclonal antibody developed by Atsushi Kawakami was obtained from the Developmental Studies Hybridoma Bank developed under the auspices of the NICHD and maintained by The University

of Iowa, Department of Biology, Iowa City, IA 52242, USA. *Conflict of Interest*: None declared.

References

Abbah J, Juliano SL. 2014. Altered migratory behavior of interneurons in a model of cortical dysplasia: the influence of elevated $GABA_A$ activity. Cereb Cortex. 24:2297–2308.

Angevine JB Jr, Sidman RL. 1961. Autoradiographic study of cell migration during histogenesis of cerebral cortex in the mouse. Nature. 192:766–768.

Bayatti N, Moss JA, Sun L, Ambrose P, Ward JF, Lindsay S, Clowry GJ. 2008. A molecular neuroanatomical study of the developing human neocortex from 8 to 17 postconceptional weeks revealing the early differentiation of the subplate and subventricular zone. Cereb Cortex. 18:1536–1548.

Bayer SA, Altman J, Dai XF, Humphreys L. 1991. Planar differences in nuclear area and orientation in the subventricular and intermediate zones of the rat embryonic neocortex. J Comp Neurol. 307: 487–498.

Borrell V, Reillo I. 2012. Emerging roles of neural stem cells in cerebral cortex development and evolution. Dev Neurobiol. 72:955–971.

Brazel CY, Romanko MJ, Rothstein RP, Levison SW. 2003. Roles of the mammalian subventricular zone in brain development. Prog Neurobiol. 69:49–69.

Calegari F, Haubensak W, Haffner C, Huttner WB. 2005. Selective lengthening of the cell cycle in the neurogenic subpopulation of neural progenitor cells during mouse brain development. J Neurosci. 25:6533–6538.

Cattaneo E, Reinach B, Caputi A, Cattabeni F, Di Luca M. 1995. Selective in vitro blockade of neuroepithelial cells proliferation by methylazoxymethanol, a molecule capable of inducing long lasting functional impairments. J Neurosci Res. 41:640–647.

Caviness VS Jr, Nowakowski RS, Bhide PG. 2009. Neocortical neurogenesis: morphogenetic gradients and beyond. Trends Neurosci. 32:443–450.

Caviness VS Jr, Takahashi T, Nowakowski RS. 1995. Numbers, time and neocortical neuronogenesis: a general developmental and evolutionary model. Trends Neurosci. 18:379–383.

Charrier C, Joshi K, Coutinho-Budd J, Kim JE, Lambert N, de Marchena J, Jin WL, Vanderhaeghen P, Ghosh A, Sassa T et al. 2012. Inhibition of SRGAP2 function by its human-specific paralogs induces neoteny during spine maturation. Cell. 149:923–935.

Charvet CJ, Striedter GF. 2011. Causes and consequences of expanded subventricular zones. Eur J Neurosci. 34:988–993.

Chenn A, Walsh CA. 2003. Increased neuronal production, enlarged forebrains and cytoarchitectural distortions in beta-catenin overexpressing transgenic mice. Cereb Cortex. 13:599–606.

Chenn A, Walsh CA. 2002. Regulation of cerebral cortical size by control of cell cycle exit in neural precursors. Science. 297: 365–369.

Costa MR, Kessaris N, Richardson WD, Gotz M, Hedin-Pereira C. 2007. The marginal zone/layer I as a novel niche for neurogenesis and gliogenesis in developing cerebral cortex. J Neurosci. 27: 11376–11388.

Dahmane N, Ruiz i Altaba A. 1999. Sonic hedgehog regulates the growth and patterning of the cerebellum. Development. 126: 3089–3100.

Dahmane N, Sanchez P, Gitton Y, Palma V, Sun T, Beyna M, Weiner H, Ruiz i Altaba A. 2001. The Sonic Hedgehog-Gli pathway regulates dorsal brain growth and tumorigenesis. Development. 128: 5201–5212.

DeFelipe J, Alonso-Nanclares L, Arellano JI. 2002. Microstructure of the neocortex: comparative aspects. J Neurocytol. 31:299–316.

Dehay C, Giroud P, Berland M, Smart I, Kennedy H. 1993. Modulation of the cell cycle contributes to the parcellation of the primate visual cortex. Nature. 366:464–466.

Dehay C, Horsburgh G, Berland M, Killackey H, Kennedy H. 1989. Maturation and connectivity of the visual cortex in monkey is altered by prenatal removal of retinal input. Nature. 337:265–267.

Dehay C, Kennedy H. 2007. Cell-cycle control and cortical development. Nat Rev Neurosci. 8:438–450.

Dehay C, Savatier P, Cortay V, Kennedy H. 2001. Cell-cycle kinetics of neocortical precursors are influenced by embryonic thalamic axons. J Neurosci. 21:201–214.

Englund C, Fink A, Lau C, Pham D, Daza RA, Bulfone A, Kowalczyk T, Hevner RF. 2005. Pax6, Tbr2, and Tbr1 are expressed sequentially by radial glia, intermediate progenitor cells, and postmitotic neurons in developing neocortex. J Neurosci. 25:247–251.

Ferrer I, Puig B, Goutan E, Gombau L, Munoz-Canoves P. 2001. Methylazoximethanol acetate-induced cell death in the granule cell layer of the developing mouse cerebellum is associated with caspase-3 activation, but does not depend on the tissue-type plasminogen activator. Neurosci Lett. 299:77–80.

Fietz SA, Kelava I, Vogt J, Wilsch-Brauninger M, Stenzel D, Fish JL, Corbeil D, Riehn A, Distler W, Nitsch R et al. 2010. OSVZ progenitors of human and ferret neocortex are epithelial-like and expand by integrin signaling. Nat Neurosci. 13:690–699.

Garcia-Moreno F, Vasistha NA, Trevia N, Bourne JA, Molnar Z. 2012. Compartmentalization of cerebral cortical germinal zones in a lissencephalic primate and gyrencephalic rodent. Cereb Cortex. 22:482–492.

Germano IM, Sperber EF. 1998. Transplacentally induced neuronal migration disorders: an animal model for the study of epilepsies. J Neurosci Res. 15:473–488.

Hansen DV, Lui JH, Parker PR, Kriegstein AR. 2010. Neurogenic radial glia in the outer subventricular zone of human neocortex. Nature. 464:554–561.

Hardan AY, Jou RJ, Keshavan MS, Varma R, Minshew NJ. 2004. Increased frontal cortical folding in autism: a preliminary MRI study. Psychiatry Res. 131:263–268.

Hasling TA, Gierdalski M, Jablonska B, Juliano SL. 2003. A radialization factor in normal cortical plate restores disorganized radial glia and disrupted migration in a model of cortical dysplasia. Eur J Neurosci. 17:467–480.

Haubensak W, Attardo A, Denk W, Huttner WB. 2004. Neurons arise in the basal neuroepithelium of the early mammalian telencephalon: a major site of neurogenesis. Proc Natl Acad Sci USA. 101: 3196–3201.

Haydar TF, Kuan CY, Flavell RA, Rakic P. 1999. The role of cell death in regulating the size and shape of the mammalian forebrain. Cereb Cortex. 9:621–626.

Hendzel MJ, Wei Y, Mancini MA, Van Hooser A, Ranalli T, Brinkley BR, Bazett-Jones DP, Allis CD. 1997. Mitosis-specific phosphorylation of histone H3 initiates primarily within pericentromeric heterochromatin during G2 and spreads in an ordered fashion coincident with mitotic chromosome condensation. Chromosoma. 106:348–360.

Hevner RF, Haydar TF. 2012. The (not necessarily) convoluted role of basal radial glia in cortical neurogenesis. Cereb Cortex. 22:465–468.

Hill J, Dierker D, Neil J, Inder T, Knutsen A, Harwell J, Coalson T, Van Essen D. 2010. A surface-based analysis of hemispheric asymmetries and folding of cerebral cortex in term-born human infants. J Neurosci. 30:2268–2276.

Holm PC, Mader MT, Haubst N, Wizenmann A, Sigvardsson M, Gotz M. 2007. Loss- and gain-of-function analyses reveal targets of Pax6 in the developing mouse telencephalon. Mol Cell Neurosci. 34: 99–119.

Ip BK, Wappler I, Peters H, Lindsay S, Clowry GJ, Bayatti N. 2010. Investigating gradients of gene expression involved in early human cortical development. J Anat. 217:300–311.

Jackson CA, Peduzzi JD, Hickey TL. 1989. Visual cortex development in the ferret. I. Genesis and migration of visual cortical neurons. J Neurosci. 9:1242–1253.

Johnston MV, Coyle JT. 1979. Histological and neurochemical effects of fetal treatment with methylazoxymethanol on rat neocortex in adulthood. Brain Res. 170:135–155.

Juliano SL, Palmer SL, Sonty RV, Noctor S, Hill GF II. 1996. Development of local connections in ferret somatosensory cortex. J Comp Neurol. 374:259–277.

Kelava I, Reillo I, Murayama AY, Kalinka AT, Stenzel D, Tomancak P, Matsuzaki F, Lebrand C, Sasaki E, Schwamborn JC et al. 2012. Abundant occurrence of basal radial glia in the subventricular zone

of embryonic neocortex of a lissencephalic primate, the common marmoset *Callithrix jacchus*. Cereb Cortex. 22:469–481.
Kerjan G, Gleeson JG. 2007. Genetic mechanisms underlying abnormal neuronal migration in classical lissencephaly. Trends Genet. 23:623–630.
Kornack DR, Rakic P. 1998. Changes in cell-cycle kinetics during the development and evolution of primate neocortex. Proc Natl Acad Sci USA. 95:1242–1246.
Kowalczyk T, Pontious A, Englund C, Daza RA, Bedogni F, Hodge R, Attardo A, Bell C, Huttner WB, Hevner RF. 2009. Intermediate neuronal progenitors (basal progenitors) produce pyramidal-projection neurons for all layers of cerebral cortex. Cereb Cortex. 19:2439–2450.
Kriegstein A, Noctor S, Martinez-Cerdeno V. 2006. Patterns of neural stem and progenitor cell division may underlie evolutionary cortical expansion. Nat Rev Neurosci. 7:883–890.
Kuida K, Haydar TF, Kuan CY, Gu Y, Taya C, Karasuyama H, Su MS, Rakic P, Flavell RA. 1998. Reduced apoptosis and cytochrome c-mediated caspase activation in mice lacking caspase 9. Cell. 94:325–337.
Kulynych JJ, Luevano LF, Jones DW, Weinberger DR. 1997. Cortical abnormality in schizophrenia: an in vivo application of the gyrification index. Biol Psychiatry. 41:995–999.
Lui JH, Hansen DV, Kriegstein AR. 2011. Development and evolution of the human neocortex. Cell. 146:18–36.
Lukaszewicz A, Cortay V, Giroud P, Berland M, Smart I, Kennedy H, Dehay C. 2006. The concerted modulation of proliferation and migration contributes to the specification of the cytoarchitecture and dimensions of cortical areas. Cereb Cortex. 16 (Suppl 1):i26–i34.
Lukaszewicz A, Savatier P, Cortay V, Giroud P, Huissoud C, Berland M, Kennedy H, Dehay C. 2005. G1 phase regulation, area-specific cell cycle control, and cytoarchitectonics in the primate cortex. Neuron. 47:353–364.
Martinez-Cerdeno V, Cunningham CL, Camacho J, Antczak JL, Prakash AN, Cziep ME, Walker AI, Noctor SC. 2012. Comparative analysis of the subventricular zone in rat, ferret and macaque: evidence for an outer subventricular zone in rodents. PLoS One. 7:e30178.
Martinez-Cerdeno V, Noctor SC, Kriegstein AR. 2006. The role of intermediate progenitor cells in the evolutionary expansion of the cerebral cortex. Cereb Cortex. 16 (Suppl 1):i152–i161.
McConnell SK, Kaznowski CE. 1991. Cell cycle dependence of laminar determination in developing neocortex. Science. 254:282–285.
McLaughlin DF, Sonty RV, Juliano SL. 1998. Organization of the forepaw representation in ferret somatosensory cortex. Somatosens Mot Res. 15:253–268.
McSherry GM. 1984. Mapping of cortical histogenesis in the ferret. J Embryol Exp Morphol. 81:239–252.
McSherry GM, Smart IH. 1986. Cell production gradients in the developing ferret isocortex. J Anat. 144:1–14.
Miyata T, Kawaguchi A, Saito K, Kawano M, Muto T, Ogawa M. 2004. Asymmetric production of surface-dividing and non-surface-dividing cortical progenitor cells. Development. 131:3133–3145.
Molnar Z. 2011. Evolution of cerebral cortical development. Brain Behav Evol. 78:94–107.
Neal J, Takahashi M, Silva M, Tiao G, Walsh CA, Sheen VL. 2007. Insights into the gyrification of developing ferret brain by magnetic resonance imaging. J Anat. 210:66–77.
Nieto M, Monuki ES, Tang H, Imitola J, Haubst N, Khoury SJ, Cunningham J, Gotz M, Walsh CA. 2004. Expression of Cux-1 and Cux-2 in the subventricular zone and upper layers II-IV of the cerebral cortex. J Comp Neurol. 479:168–180.
Noctor SC, Martinez-Cerdeno V, Ivic L, Kriegstein AR. 2004. Cortical neurons arise in symmetric and asymmetric division zones and migrate through specific phases. Nat Neurosci. 7:136–144.
Noctor SC, Martinez-Cerdeno V, Kriegstein AR. 2008. Distinct behaviors of neural stem and progenitor cells underlie cortical neurogenesis. J Comp Neurol. 508:28–44.
Noctor SC, Palmer SL, Hasling T, Juliano SL. 1999. Interference with the development of early generated neocortex results in disruption of radial glia and abnormal formation of neocortical layers. Cereb Cortex. 9:121–136.
Noctor SC, Palmer SL, McLaughlin DF, Juliano SL. 2001. Disruption of layers 3 and 4 during development results in altered thalamocortical projections in ferret somatosensory cortex. J Neurosci. 21: 3184–3195.
Noctor SC, Scholnicoff NJ, Juliano SL. 1997. Histogenesis of ferret somatosensory cortex. J Comp Neurol. 387:179–193.
O'Leary DD. 1989. Do cortical areas emerge from a protocortex? Trends Neurosci. 12:400–406.
Palmer SL, Noctor SC, Jablonska B, Juliano SL. 2001. Laminar specific alterations of thalamocortical projections in organotypic cultures following layer 4 disruption in ferret somatosensory cortex. Eur J Neurosci. 13:1559–1571.
Penschuck S, Flagstad P, Didriksen M, Leis M, Michael-Titus AT. 2003. Decrease in parvalbumin-expressing neurons in the hippocampus and increased phencyclidine-induced locomotor activity in the rat methylazoxymethanol (MAM) model of schizophrenia. Eur J Neurosci. 23:279–284.
Pilaz LJ, Patti D, Marcy G, Ollier E, Pfister S, Douglas RJ, Betizeau M, Gautier E, Cortay V, Doerflinger N et al. 2009. Forced G1-phase reduction alters mode of division, neuron number, and laminar phenotype in the cerebral cortex. Proc Natl Acad Sci USA. 106: 21924–21929.
Polleux F, Dehay C, Goffinet A, Kennedy H. 2001. Pre- and post-mitotic events contribute to the progressive acquisition of area-specific connectional fate in the neocortex. Cereb Cortex. 11:1027–1039.
Poluch S, Jablonska B, Juliano SL. 2008. Alteration of interneuron migration in a ferret model of cortical dysplasia. Cereb Cortex. 18:78–92.
Poluch S, Juliano SL. 2010. Populations of radial glial cells respond differently to reelin and neuregulin1 in a ferret model of cortical dysplasia. PLoS One. 5:e13709.
Pramparo T, Youn YH, Yingling J, Hirotsune S, Wynshaw-Boris A. 2010. Novel embryonic neuronal migration and proliferation defects in Dcx mutant mice are exacerbated by Lis1 reduction. J Neurosci. 30:3002–3012.
Rabe A, Haddad R, Dumas R. 1985. Behavior and neurobehavioral teratology using the ferret. Lab Anim Sci. 35:256–267.
Rakic P. 2009. Evolution of the neocortex: a perspective from developmental biology. Nat Rev Neurosci. 10:724–735.
Rakic P. 2005. Less is more: progenitor death and cortical size. Nat Neurosci. 8:981–982.
Rakic P. 1995. A small step for the cell, a giant leap for mankind: a hypothesis of neocortical expansion during evolution. Trends Neurosci. 18:383–388.
Rakic P. 1988. Specification of cerebral cortical areas. Science. 241: 170–176.
Rash BG, Tomasi S, Lim HD, Suh CY, Vaccarino FM. 2013. Cortical gyrification induced by fibroblast growth factor 2 in the mouse brain. J Neurosci. 33:10802–10814.
Reillo I, Borrell V. 2012. Germinal zones in the developing cerebral cortex of ferret: ontogeny, cell cycle kinetics, and diversity of progenitors. Cereb Cortex. 22:2039–2054.
Reillo I, de Juan Romero C, Garcia-Cabezas MA, Borrell V. 2011. A role for intermediate radial glia in the tangential expansion of the mammalian cerebral cortex. Cereb Cortex. 21:1674–1694.
Rockel AJ, Hiorns RW, Powell TP. 1980. The basic uniformity in structure of the neocortex. Brain. 103:221–244.
Scott SI, Morris LS, Bird K, Davies RJ, Vowler SL, Rushbrook SM, Marshall AE, Laskey RA, Miller R, Arends MJ et al. 2003. A novel immunohistochemical method to estimate cell-cycle phase distribution in archival tissue: implications for the prediction of outcome in colorectal cancer. J Pathol. 201:187–197.
Sessa A, Mao CA, Hadjantonakis AK, Kein WH, Broccoli V. 2008. Tbr2 directs conversion of radial glia into basal precursors and guides neuronal amplification by indirect neurogenesis in the developing cortex. Neuron. 60:56–69.
Shitamukai A, Konno D, Matsuzaki F. 2011. Oblique radial glial divisions in the developing mouse neocortex induce self-renewing progenitors outside the germinal zone that resemble primate outer subventricular zone progenitors. J Neurosci. 31:3683–3695.

Smart IH, Dehay C, Giroud P, Berland M, Kennedy H. 2002. Unique morphological features of the proliferative zones and postmitotic compartments of the neural epithelium giving rise to striate and extrastriate cortex in the monkey. Cereb Cortex. 12:37–53.

Smart IH, McSherry GM. 1986. Gyrus formation in the cerebral cortex in the ferret. I. Description of the external changes. J Anat. 146:141–152.

Smart IH, Smart M. 1982. Growth patterns in the lateral wall of the mouse telencephalon: I. Autoradiographic studies of the histogenesis of the isocortex and adjacent areas. J Anat. 134: 273–298.

Smart IH, Smart M. 1977. The location of nuclei of different labelling intensities in autoradiographs of the anterior forebrain of postnatial mice injected with [3H]thymidine on the eleventh and twelfth days post-conception. J Anat. 123:515–525.

Stahl R, Walcher T, De Juan Romero C, Pilz GA, Cappello S, Irmler M, Sanz-Aquela JM, Beckers J, Blum R, Borrell V et al. 2013. Trnp1 regulates expansion and folding of the mammalian cerebral cortex by control of radial glial fate. Cell. 153:535–549.

Tarabykin V, Stoykova A, Usman N, Gruss P. 2001. Cortical upper layer neurons derive from the subventricular zone as indicated by Svet1 gene expression. Development. 128:1983–1993.

Tarui T, Takahashi T, Nowakowski RS, Hayes NL, Bhide PG, Caviness VS. 2005. Overexpression of p27 Kip 1, probability of cell cycle exit, and laminar destination of neocortical neurons. Cereb Cortex. 15:1343–1355.

Vaccarino FM, Schwartz ML, Raballo R, Nilsen J, Rhee J, Zhou M, Doetschman T, Coffin JD, Wyland JJ, Hung YT. 1999. Changes in cerebral cortex size are governed by fibroblast growth factor during embryogenesis. Nat Neurosci. 2:246–253.

Van den Berg HW, Ball CR. 1972. The effect of methylazoxymethanol acetate on DNA synthesis and cell proliferation of synchronous HeLa cells. Mutat Res. 16:381–390.

Van der Loos H, Woolsey TA. 1973. Somatosensory cortex: structural alterations following early injury to sense organs. Science. 179: 395–398.

Wang X, Tsai JW, LaMonica B, Kriegstein AR. 2011. A new subtype of progenitor cell in the mouse embryonic neocortex. Nat Neurosci. 14:555–561.

Yingling J, Youn YH, Darling D, Toyo-Oka K, Pramparo T, Hirotsune S, Wynshaw-Boris A. 2008. Neuroepithelial stem cell proliferation requires LIS1 for precise spindle orientation and symmetric division. Cell. 132:474–486.

Zecevic N, Chen Y, Filipovic R. 2005. Contributions of cortical subventricular zone to the development of the human cerebral cortex. J Comp Neurol. 491:109–122.

Zilles K, Armstrong E, Moser KH, Schleicher A, Stephan H. 1989. Gyrification in the cerebral cortex of primates. Brain Behav Evol. 34:143–150.

Zimmer C, Tiveron MC, Bodmer R, Cremer H. 2004. Dynamics of Cux2 expression suggests that an early pool of SVZ precursors is fated to become upper cortical layer neurons. Cereb Cortex. 14:1408–1420.